NUCLEAR MAGNETIC RESONANCE STUDIES

OF

FERROELECTRIC AMMONIUM SULFATE AND FLUOROBERYLLATE

NUCLEAR MAGNETIC RESONANCE STUDIES
OF
FERROELECTRIC AMMONIUM SULFATE AND FLUOROBERYLLATE

By

DONALD WILLIAM KYDON, B.A., M.Sc.

A Thesis
Submitted to the Faculty of Graduate Studies
in Partial Fulfilment of the Requirements
for the Degree
Doctor of Philosophy

McMaster University
November 1968

DOCTOR OF PHILOSOPHY (1968)
(Physics)

McMASTER UNIVERSITY
Hamilton, Ontario

TITLE: Nuclear Magnetic Resonance Studies of Ferroelectric Ammonium Sulfate and Fluoroberyllate

AUTHOR: Donald William Kydon, B.A. (Johns Hopkins University)
M.Sc.(McMaster University)

SUPERVISOR: Professor H. E. Petch, Vice-President, Academic
University of Waterloo

NUMBER OF PAGES: viii, 104

SCOPE AND CONTENTS:

The temperature dependences of the deuteron spin-lattice relaxation times, T_1, in ferroelectric ammonium sulfate, $(ND_4)_2SO_4$, and ammonium fluoroberyllate, $(ND_4)_2BeF_4$, have been studied by transient methods over the range 80 to 475°K. The ability to resolve the individual correlations of the two independent ND_4 groups in the deuteron experiment has thrown new light on the reorientation of the ammonium groups and their behaviour in the phase transition.

It has been proposed that the mechanism of the phase transition in ammonium sulfate is a disordering, with respect to the a b plane in the paraelectric phase, of the ND_4 dipoles which also make the dominant contribution to the spontaneous polarization. The present N.M.R. results show that in $(ND_4)_2SO_4$, T_1 at both non-equivalent ND_4 groups is affected at the phase transition, whereas in $(ND_4)_2BeF_4$, it is affected at only one ND_4 group. This suggests that the phase transitions in these two

materials are rather different and that in ammonium sulfate both types of ammonium ions are involved whereas in ammonium fluoroberyllate only one type is involved in the transition. Such a conclusion is supported by evidence from measurements of thermal and dielectric properties.

An earlier study of the proton spectrum in $(NH_4)_2SO_4$ reported a value of 33 gauss^2 for the second moment at 20°K. This is considerably smaller than the expected rigid lattice value of 50 gauss^2 and it was concluded that while some of the NH_4^+ groups are effectively rigid at 20°K others are still reorienting. Our new results for the proton second moment confirm the low value down to 4.2°K but our results for T_1 indicate that the proton line is not motionally narrowed.

ACKNOWLEDGEMENTS

I would like to thank Professor H. E. Petch for suggesting so interesting a thesis topic, and for his hospitality offered throughout the course of the work.

It is a pleasure to thank Dr. M. M. Pintar whose understanding of both the theoretical and experimental aspects of N.M.R. led to a positive direction of the experiment. I am greatly indebted to Stane Vrscaj for designing a very flexible spectrometer necessary in this work. Thanks are due to Arthur Watton for the many valuable discussions concerning relaxation theory, and to Allan Sharp who helped analyze the experimental data. Also, I should like to express my appreciation to my family, especially my wife Motria, for consistent patience and encouragement.

This research was made possible by grants-in-aid to Professor Petch from both the National Research Council and the Defence Research Board of Canada. I am grateful for the financial support given me by the Province of Ontario in the form of an Ontario Graduate Fellowship.

TABLE OF CONTENTS

LIST OF FIGURES

LIST OF TABLES

CHAPTER I

INTRODUCTION

I.1 Background Survey:

Since the discovery of Nuclear Magnetic Resonance (N.M.R.) (Purcell, Torrey and Pound (1); Bloch, Hansen and Packard (2)) in 1945, the N.M.R. technique has been developed into a powerful tool for studying the internal structure and properties of matter in the gaseous, liquid and solid states.

The N.M.R. principle depends on the fact that when an ensemble of nuclear magnets is placed in a magnetic field H_o, their orientational energies with respect to H_o are quantized. These so-called Zeeman levels have energies given by $mg\mu_N H_o$, where m, g, μ_N are the magnetic quantum number, nuclear g-factor and nuclear magneton respectively. The values taken by m range from I, I-1, ...-I, where I is the nuclear spin. The relative populations of the Zeeman levels are governed by the well known Boltzmann factor $\exp(-\Delta E/kT)$ where $\Delta E = g\mu_N H_o$. Transitions may be induced under the correct resonance and polarization conditions by a time varying magnetic field. These transitions among the various Zeeman levels are governed by the magnetic dipole selection rule $\Delta m = \pm 1$. Because of the Boltzmann factor, there will be a fraction $\exp(\Delta E/kT)$ more nuclei in the lower Zeeman state; consequently there will be a correspondingly larger amount of absorption than emission of electromagnetic energy. The experimental arrangement which observes this absorption of energy is called the continuum wave (cw) technique.

It is clear that the population difference on which the cw technique is based would very soon disappear were it not for spin-lattice coupling. By the lattice we shall mean all other degrees of freedom of the atomic system. It is this coupling which enables the nuclei in higher energy states, to give up their energy and return to a lower energy state, and, as a consequence, preserve the equilibrium distribution. The coupling of the spin system to the lattice may be observed by switching off the resonant oscillating field for a specific time and then turning it back on and observing the change in the magnetization. The observation of the time dependent nuclear magnetization forms the basis of the transient technique. The experimental arrangement which monitors the spin-lattice coupling yields the useful parameter, T_1, the spin lattice relaxation time.

It should also be noted that the nuclear spins are coupled to one another as well as to the lattice. This coupling leads to a broadening of the absorption spectrum the width of which can be related to the parameter, T_2, the spin-spin relaxation time.

For nearly two decades N.M.R. techniques have been applied successfully to problems of structure and motion of atoms and molecules in the solid state. Structural studies of protons have been by far the most numerous. Although X-ray diffraction accurately determines the positions of other atoms in a crystal lattice, little precise information normally can be obtained for hydrogen atoms since they scatter X-rays very weakly. On the other hand, protons are very sensitive to the N.M.R. technique because of their large magnetic moment. A proton resonance study can often complete a structure in which the heavy atom positions have been determined by the X-ray method. In other words, the two techniques are complementary.

The factor in the dipolar Hamiltonian which gives rise to the observed dipolar-broadened spectrum is $(1 - 3\cos^2\theta)r^{-3}$ for each pair of nuclei in the system, where r is the internuclear vector and θ is the angle between r and the applied field H_o. The r^{-3} dependence on distance makes it clear that interactions between nearest neighbours will give the largest contribution. Furthermore, these interactions are highly anisotropic. A single crystal study will give the maximum information; however, internuclear distances can often be obtained from a powder study although the angular dependence is lost.

Because of the complexity or in most cases the impossibility of completely determining the spectrum, it is more useful to work with the second moment or mean square width of the spectrum. A theoretical value of the second moment may be calculated assuming a model and compared with that observed. The general correctness of the model may be established, and if the model does not contain too many unknown parameters, these may be determined.

Any form of atomic or molecular motion in the crystal is liable to modify the spectrum and its 2nd moment, often quite dramatically. The angular factor $(1 - 3\cos^2\theta)$ in each term of the dipolar Hamiltonian is no longer a constant; the mean interaction is in general reduced by the motion, and as a result the spectrum is narrower. The amount of the narrowing, and the reduction of the observed 2nd moment, can be expressed quantitatively, and usually enables the nature of the motion to be established.

The dynamics of the nuclear motions revealed by line width narrowing may be studied through the temperature-dependence of the spin-lattice relaxation time, T_1. The fluctuating dipolar interaction caused by the random molecular motion causes transitions through the off-diagonal terms of the dipolar Hamiltonian, and attempts to maintain thermal equilibrium between the spin system and the lattice. The efficiency of this relaxation mechanism depends on the intensity of the Fourier spectrum of the random motion at the resonance frequency and this in turn depends upon the correlation time τ of the random motion. At temperatures where τ^{-1} is of the same order as the resonance frequency this relaxation mechanism is most effective and T_1 has its minimum value. At either higher or lower temperatures T_1 is larger. From the theoretical dependence of T_1 on τ, measurements of the temperature dependence of τ can be deduced and often fit a simple activation law.

In the case when the nucleus under investigation has an electric quadrupole moment ($I > 1/2$), spin-lattice relaxation may be effected either through a fluctuating magnetic interaction or through the interaction of the quadrupole moment with the fluctuating crystalline electric field. The quadrupole interaction dominates except in the cases when the electric field gradient vanishes as at a site of cubic symmetry, or the sample is heavily contaminated by paramagnetic impurities.

Much detailed information concerning the motion of atoms and molecules has been extracted from the application of N.M.R. to solids. Molecular rotation is quite common which however is almost never free, but consists rather in the reorientation of the molecule or atomic group between a number of equilibrium positions. The nature of the rotational motion can usually be established. One can determine whether the whole molecule reorients or only a part of it, and whether the motion is about one axis or is more general. The temperature-dependence of the rate of the motion can generally be determined. The diffusion of atoms, ions and molecules can be detected, and in favourable cases the rate of migration and its temperature dependence may be determined. Since this information is extracted from two pieces of experimental data, namely the absorption spectrum and the spin-lattice relaxation time, a full investigation of any solid will embrace measurements of both over as wide a range of temperature as possible.

It is the application of N.M.R. to the dynamic situation in two ferroelectric crystals that forms the basis of this thesis. Although the phenomenon of ferroelectricity has been extensively studied in recent years, much remains to be understood about the atomic mechanism. X-ray, neutron diffraction, thermal and dielectric studies of ferroelectric crystals are very helpful in improving this situation but N.M.R. techniques also can make important contributions. The resonance signal of a nucleus in a crystal depends strongly upon the particular state of the crystal and therefore may be used to detect and study the progress of phase transitions even when the actual atomic displacements are very small. Furthermore, in hydrogen bonded crystals, where the interproton distances are only slightly greater than the distances over which proton motion occurs, N.M.R. may clarify the role of the hydrogen atoms in the ferroelectric transition.

I.2 Ammonium Sulfate and Ammonium Fluoroberyllate:

The ferroelectric property of ammonium sulfate, $(NH_4)_2SO_4$, below 223°K and of ammonium fluoroberyllate, $(NH_4)_2BeF_4$, below 176°K were discovered by Matthias and Remeika (3) and by Pepinsky and Jona (4), respectively. Although both are ferroelectric and originally were believed to be isomorphic in structure, they have been found to differ in a number of important aspects. The crystal symmetries of the two materials are different in both their paraelectric and ferroelectric phases and the polar axes in the ferroelectric phases develop along different crystallographic axes.

An early (1958) thermal study of $(NH_4)_2SO_4$ and $(NH_4)_2BeF_4$ by Hoshino et al.(5) indicated that the mechanism of the phase transitions of these two crystals are of a different type. There is evidence of latent heat in the $(NH_4)_2SO_4$ transition, whereas $(NH_4)_2BeF_4$ exhibits a broad peak at the transition which suggests a second-order transition. From a study of the dielectric constant these authors reported that the shape of the ε vs T curves of $(NH_4)_2SO_4$ and $(NH_4)_2BeF_4$ is rather unusual for a ferroelectric transition. The Curie-Weiss law was not obeyed above the transition temperature, unlike most of the ferroelectrics known at that time. However, a more recent dielectric, spontaneous polarization and specific heat study of $(NH_4)_2BeF_4$ by Strukov et al.(6) in a narrow range around the transition indicated that the transition is first order.

In an early proton N.M.R. study (1960), Blinc and Levstek (7) found that $(NH_4)_2SO_4$ and $(NH_4)_2BeF_4$ which have very similar absorption lines at room temperature, showed an entirely different behaviour at low temperatures. In $(NH_4)_2BeF_4$ the 2nd moment of the proton absorption line increases very slightly between 423 and 93°K where it attains the value of 8 gauss^2. The expected rigid lattice value for an ammonium group is about 50 gauss^2. The 2nd moment value of 8 gauss^2 at 93°K demonstrated the complete disappearance of the intra- NH_4^+ magnetic interactions due to the random reorientations of the NH_4^+ ions. The potential barrier hindering the movement of the ammonium ions appeared to be low. On the other hand in $(NH_4)_2SO_4$ the 2nd moment of the proton absorption line increased from the value of 6 gauss^2 to 28 gauss^2 below 163°K. The absorption line split into two well resolved components. They interpreted these results in terms of the broad band arising from "frozen-in" ammonium ion protons and the narrow band from rapidly reorienting ammonium ions. Their IR studies indicated the existence of deformation in the NH_4, SO_4, and BeF_4 groups in the ferroelectric phase and from this they underlined the importance of the N-H...O and N-H... F hydrogen bonds in the transition.

In 1960 from a proton line-width study, Richards and Schaefer (8) reported a 2nd moment value for $(NH_4)_2SO_4$ at 20°K of 33 gauss^2 which is again below the value expected for rigid ammonium groups. They explained the 2nd moment and line shape of the derivative curve below the line width transition on the assumption that two-thirds of the ions are rigid while the others are in motion. They assumed that the minor peaks in the derivative curve at 20°K arise from rigid ions and that the central peaks are due to ions in motion. The derivative curve was then treated as a superposition of two such curves, one due to the outer peaks (40 gauss^2) and one due to the central peaks (6 gauss^2).

From an early spin-lattice relaxation study (1962), Miller et al.(9) reported that $(NH_4)_2SO_4$ displays a marked discontinuity in the proton T_1

at the ferroelectric transition. T_1 abruptly decreases from 1 sec. to 300 msec. which they interpreted as a large change in the rate of NH_4^+ motion on going to the ferroelectric phase. The slope of the proton T_1 vs 1/T curve was found to change and from the slope they calculated that the potential hindering the NH_4^+ reorientation to be 2.3 kcal/mole in the paraelectric phase and 6.1 kcal/mole in the ferroelectric phase. In the case of $(NH_4)_2BeF_4$ no discontinuity was reported but only a change in the slope of the proton T_1 vs 1/T curve. From the slope, the hindering potential was calculated to be 1.5 kcal/mole in the paraelectric phase and 5.3 kcal/mole in the ferroelectric phase. They concluded from these data that the barrier to NH_4^+ rotation is higher in the ferroelectric than the paraelectric phase and that the change to the ferroelectric phase involves a change in lattice structure and hence alters the effective potential against which the motion occurs. Unfortunately, due to the rather narrow temperature range over which the experiment was carried out, the results are not complete.

In a much more recent spin-lattice relaxation study (1967), O'Reilly and Tsang (10), (11) reported results only in approximate agreement with those of Miller et al. Their observation of two minima in the proton T_1 vs 1/T curve was interpreted in terms of two non-equivalent NH_4^+ (Type I and Type II) tetrahedra rotating at different frequencies and coupled to each other via the dipole-dipole interaction. In the case of $(NH_4)_2BeF_4$ they found that both the proton and fluorine spin-lattice relaxation become markedly non-exponential over certain temperature ranges. For $(NH_4)_2SO_4$, which contains protons at two chemically inequivalent sites at which relaxation processes are different, only exponential relaxation processes were observed. In $(NH_4)_2SO_4$ it was found that between the ferroelectric and paraelectric phases the activation energy decreases by 40% for the Type I ion and 15% for Type II. In the case of $(NH_4)_2BeF_4$ the change in activation energy in going through the transition was found to be very small.

Deuteron magnetic resonance data for $(ND_4)_2SO_4$(10) suggested that the tilt of the ammonium dipoles is symmetrical with respect to the a b plane in the ferroelectric phase. The mechanism of the phase transition is the disordering of the ammonium dipoles with respect to the ab plane. Similar data for $(ND_4)_2BeF_4$(11) indicated that the transition is due to a tilting of the ammonium ions either parallel or anti-parallel to the ferroelectric axis.

A neutron diffraction study of the structures of ferroelectric and paraelectric $(NH_4)_2SO_4$ has been carried out (1966) by Schlemper and Hamilton (12). Their results agreed with inelastic neutron scattering studies, Rush and Taylor (13), that the rotational freedom of the ammonium ions undergoes little change in passing through the transition. These results are not consistent with the N.M.R. studies of Miller et al.(9). Also the interpretation given by Richards and Schaefer (8) is ruled out from the symmetry requirement that there be equal numbers of two independent ammonium ions in the structure. They suggest that the transition is not of the order-disorder type, but rather involves a change in the hydrogen bonding of the ammonium ions to the sulfate ions which results in stronger hydrogen bonds in the ferroelectric phase. At room temperature the ammonium ions are highly distorted with the H-N-H angles varying from 104.7° to 118.5° in one ammonium ion, and from 100.2°

to 116.2° in the other ammonium ion. In the ferroelectric phase the ammonium ions are less distorted, with the H-N-H angles varying from 106.1° to 111.6° in one ammonium ion and from 104.7° to 114.1° in the other ammonium ion. The transition then results in stronger hydrogen bonds and less distorted ammonium ions, both of which seem to be energetically favourable.

I.3 Scope of the Present Work:

From the foregoing discussion of the published material on ammonium sulfate and fluoroberyllate it is evident that many aspects of the atomic nature of the ferroelectric phase transition and the behaviour of the ammonium groups at the transition are not clearly understood. It is convenient to summarize those difficulties which could perhaps be resolved by an appropriate N.M.R. study.

Early spin-lattice relaxation studies in ammonium sulfate (9) indicated that there is a significant change in the hindering potential for NH_4^+ reorientation upon entering the ferroelectric phase. They suggested that the change to the ferroelectric phase involves a change in lattice structure and hence alters the effective potential against which the motion occurs. These findings are not in agreement with neutron studies (12,13) which indicated little change in the hindering potential upon passing into the ferroelectric phase. Proton spin-lattice relaxation studies (10, 11) in both materials suggested that relaxation was brought about by the reorientation of two non-equivalent NH_4 groups, although individual correlations could not be resolved. A proposed model based on deuteron magnetic absorption results (10, 11), that the ferroelectric phase comes about because of tilting of the ammonium dipoles along the ferroelectric axes, is in good agreement with dielectric and thermal data (5). There is at present little known about the nature of the phase transition in ammonium fluoroberyllate although O'Reilly, Peterson and Tsang (11) suggest that it will be very similar to sulfate. As a result of extensive studies a fairly clear picture of the ferroelectric mechanism in $(NH_4)_2SO_4$ is beginning to emerge but much more needs to be done to bring our understanding of $(NH_4)_2BeF_4$ to an equivalent point.

With the foregoing in mind we decided to carry out a deuteron relaxation experiment on both of these materials over the widest possible temperature range. In the first place this would give still another opportunity to study the hindering potential across the transition. Furthermore, since the deuteron possesses an electric quadrupole moment it would be expected to be much more tightly coupled to the lattice leading to shorter T_1's. The quadrupole coupling combined with ND_4 reorientations could lower T_1 to a value where under certain conditions it might be smaller than the spin-diffusion times. In the light of the foregoing, it was hoped that such an experiment would be able to resolve the correlations of the two independent ammonium groups. Should this prove possible a study of the individual correlations at the transition would not only yield information concerning the nature of the transition in ammonium fluoroberyllate but would also provide additional data on both materials which could then be compared with results already available.

It should also be noted that the mechanism responsible for the proton line narrowing in $(NH_4)_2SO_4$ at very low temperatures is presently still not understood. Attempts to explain the narrowing in terms of reorientation of a fraction of the total number of groups have been shown to be inconsistent with other known data (12). As a result we decided to check the earlier second moment analysis and to extend the proton spin-lattice relaxation study down to 4.2^oK in case there was a line-width transition at temperatures lower than other workers had reached. It was hoped that from the knowledge of the relaxation rate at very low temperatures we could decide whether or not motion was the cause of line narrowing at these temperatures.

CHAPTER II

THEORY

II.1 Introduction:

We are interested in a quantum-mechanical description of the coupling of the spin system S with all other degrees of freedom, called the lattice. Of particular interest is the form of the spin-lattice relaxation time for dipolar and quadrupolar couplings. In an attempt to increase the coherence of the presentation, the physical system will first be described in general terms from which the particular expressions may be obtained with relative ease. Since there is no claim to originality in this section, the notation used is that which is found in Abragam (14).

II.2 The Density Matrix:*

In order to simplify the discussion we will treat quantum-mechanically only the spin system S assuming that the lattice is classical and has an infinite temperature. At the end of the discussion the appropriate Boltzmann weighting will be introduced.

This procedure can be justified on purely quantum-mechanical arguments (14).

We begin by considering the Hamiltonian $\hbar \mathcal{H}_0 + \hbar \mathcal{H}_1(t)$. Here, $\hbar \mathcal{H}_0$ is the main or Zeeman Hamiltonian and $\hbar \mathcal{H}_1(t)$ is the perturbing

---

* Throughout the text $\hbar$ is used in place of $h/2\pi$.

Hamiltonian which describes the coupling of the spin system with the lattice and is a stationary random operator. [Appendix A]

The equation of motion for the density matrix σ [Appendix B] for the spin system S is:

$$\frac{d\sigma}{dt} = - i[H_o + H_1(t), \sigma] \tag{2.1}$$

To exhibit the slow variation of the observables due to the coupling of the system S with the lattice rather than the fast motion due to the main Hamiltonian $h\, H_o$, we introduce the interaction representation:

$$\sigma^* = e^{iH_o t} \sigma e^{-iH_o t} \qquad \text{and} \qquad H_1{}^*(t) = e^{iH_o t} H_1(t) e^{-iH_o t}$$

Substituting the above into equation (2.1) we obtain:

$$\frac{d\sigma^*}{dt} = - i[H_1{}^*(t), \sigma^*] \tag{2.2}$$

Integrating equation (2.2) by iteration up to the 2nd order:

$$\sigma^*(t) = \sigma^*(0) - i \int_o^t [H_1{}^*(t'),\sigma^*(0)]dt' - \int_o^t dt' \int_o^{t'} dt''[H_1{}^*(t'),[H_1^*(t''),\sigma^*(0)]] \tag{2.3}$$

Differentiating equation (2.3):

$$\frac{d\sigma^*}{dt} = - i[H_1{}^*(t),\sigma^*(0)] - \int_o^t dt' \; [H_1{}^*(t), \; [H_1{}^*(t'), \; \sigma^*(0) \;]] \tag{2.4}$$

The fact that $h\, H_1(t)$ is a stationary random operator it must depend on t only through the difference. Upon the introduction of the variable $\tau = t - t'$, equation (2.4) may be written as:

$$\frac{d\sigma^*}{dt} = - i[H_1^*(t),\sigma^*(0)] - \int_0^t d\tau\ [H_1^*(t),[H_1^*(t-\tau),\sigma^*(0)]] \qquad (2.5)$$

From equation (2.5) it is clear that $\sigma^*(t)$ is a random operator. In order to obtain the observable behaviour of a statistical ensemble of spin systems, equation (2.5) must be averaged over the random Hamiltonians $\hbar H_1(t)$. A number of assumptions will now be made which are justified because of the shortness of the correlation time of the random Hamiltonians. Without proof (14), we assume:

1. $\overline{H_1(t)} = 0$
2. it is permitted to neglect the correlation between $H_1^*(t)$ and $\sigma^*(0)$ in averaging equation (2.5) and average them separately,
3. it is permitted to replace $\sigma^*(0)$ by $\sigma^*(t)$ on the right hand side of equation (2.5),
4. it is permitted to extend the upper limit of the integral in equation (2.5) to $+\infty$,
5. it is permitted to neglect all higher-order terms in the expansion of equation (2.5).

Applying these assumptions, the first term on the right of equation (2.5) averages to zero, and, dropping the bar on σ^* which from now on will stand for the average density matrix, we obtain:

$$\frac{d\sigma^*}{dt} = - \int_0^\infty d\tau\ \overline{[H_1(t),\ [H_1^*(t-\tau),\ \sigma^*(t)]\ ]} \qquad (2.6)$$

As mentioned previously it has been assumed in the present treatment that the lattice is at an infinite temperature. To correct for a finite temperature, we introduce the Boltzmann weighting factor, i.e., $\sigma^*(t)$ is replaced by $\sigma^*(t) - \sigma_o^*$ where

$$\sigma_o^* = \sigma_o = \exp(-\hbar\, H_o/kT) \;/\; \mathrm{tr}\,\{\, \exp(-\hbar\, H_o/kT)\, \}$$

II.3 The Density Matrix in Operator Form:

The next step is to cast equation (2.6) into operator form. This form will then be readily applicable to a specific spin-lattice coupling.

The random Hamiltonian $\hbar\, H_1(t)$ can be expanded as:

$$H_1(t) = \sum_q F^{(q)} A^{(q)} \tag{2.7}$$

where $F^{(q)}$ are random functions of time and $A^{(q)}$ are operators acting on the variables of the spin system.

We now introduce the correlation functions [Appendix A]

$$g_{qq'}(\tau) = \overline{F^{(q)}(t)\, F^{(q')*}(t+\tau)}$$

with the Fourier transforms:

$$J_{qq'}(\omega) = \int_{\infty}^{\infty} g_{qq'}(\tau)\, e^{-i\omega\tau} d\tau$$

and

$$j_{qq'}(\omega) = \int_{0}^{\infty} g_{qq'}(\tau)\, e^{-i\omega\tau} d\tau$$

A necessary requirement is that $\mathcal{H}_1(t)$ must be hermitian. Therefore, if $F^{(q)}$ are complex functions and $A^{(q)}$ non-hermitian operators then for each term $F^{(q)}A^{(q)}$ of our expansion there must be associated a term $F^{(q)*}A^{(q)\dagger}$. We introduce the convention $F^{(-q)} = F^{(q)*}$, $A^{(-q)} = A^{(q)\dagger}$. Finally, recalling that equation (2.6) is written in the interaction representation, the following definitions will be useful in our present expansion:

$$\left.\begin{aligned} e^{i\mathcal{H}_o t}A^{(q)}e^{-i\mathcal{H}_o t} &= A^{(q)}(t) = \sum_p A_p^{(q)}\, e^{i\omega_p^{(q)}t} \\ e^{i\mathcal{H}_o t}A^{(-q)}e^{-i\mathcal{H}_o t} &= A^{(-q)}(t) = \sum_p A_p^{(-q)}e^{i\omega_p^{(-q)}t} \\ \omega_p^{(-q)} &= -\,\omega_p^{(q)} \end{aligned}\right\} \qquad (2.8)$$

and hence,

$$\mathcal{H}_1^{\,*}(t) = e^{i\mathcal{H}_o t}\mathcal{H}_1(t)e^{-i\mathcal{H}_o t} = \sum_{p,q} F^{(q)}A_p^{(q)}e^{i\omega_p^{(q)}t} \qquad (2.9)$$

Now substitute equation (2.9) into equation (2.6):

$$\frac{d\sigma^*}{dt} = -\int_0^\infty d\tau \;\overline{\sum_{p,q,p',q'} [F^{(q')}A_{p'}^{(q')}e^{i\omega_{p'}^{(q')}t},[F^{(q)}(t-\tau)A_p^{(q)}e^{i\omega_p^{(q)}(t-\tau)},\sigma^*(t)]]}$$

which may be written as:

$$\frac{d\sigma^*}{dt} = -\sum_{p,q,p',q'} e^{i(\omega_{p'}^{(q')}+\omega_p^{(q)})t}\,[A_{p'}^{(q')},[A_p^{(q)},\sigma^*(t)]]\int_0^\infty d\tau\; \overline{F^{(q')}(t)F^{(q)}(t-\tau)e^{-i\omega_p^{(q)}\tau}}$$

(2.10)

By recalling the definition of the correlation function $g_{qq'}(\tau)$, we easily observe that the integrand on the right hand side of the equation (2.10) is simply $g_{q,-q'}(\tau)$. Assuming for simplicity $g_{qq'}(\tau) = \delta_{qq'} g_q(\tau)$ and neglecting off diagonal terms we finally obtain;

$$\frac{d\sigma^*}{dt} = - \sum_{p,q} [A_p^{(-q)},[A_p^{(q)},\sigma^*(t)]\,] \int_o^\infty g_q(\tau) e^{-i\omega_p^{(q)}\tau} d\tau \qquad (2.11)$$

It can be shown [Appendix A] that:

$$\int_o^\infty g_q(\tau) e^{-i\omega_p^{(q)}\tau} d\tau = \frac{1}{2} \int_{-\infty}^\infty g_q(\tau) e^{-i\omega_p^{(q)}\tau} d\tau - i \int_o^\infty g_q(\tau) \sin(\omega_p^{(q)}\tau) d\tau$$

$$= \frac{1}{2} J_q(\omega_p^{(q)}) - i\, k_q(\omega_p^{(q)})$$

The imaginary term leads to a small shift in energy of the spin system and can be dropped from equation (2.11). Thus we obtain:

$$\frac{d\sigma^*}{dt} = - \frac{1}{2} \sum_{p,q} J_q(\omega_p^{(q)}) \, [A_p^{(-q)}, [A_p^{(q)}, \sigma^*(t)]\,] \qquad (2.12)$$

II.4 The Macroscopic Equations:

The quantity which is observed in an experiment on a macroscopic sample containing a collection of systems S is $q(t) = \langle Q \rangle = \mathrm{tr}\,\{\sigma(t)Q\}$ [Appendix B] where Q is an operator which acts on variables of system S. It will be convenient to calculate $q^*(t) = \langle Q \rangle^* = \mathrm{tr}\,\{\sigma^*(t)Q\}$ which as mentioned previously gives the slow variation of Q due to the coupling of the spin system with the lattice. In order to obtain the equation of motion of Q multiply both sides of equation (2.6) by Q and take trace. It can be shown [Appendix C] that we get an equation of the form:

$$\frac{dq^*}{dt} = - \{a^* - a_o\} \tag{2.13}$$

where

$$a^* = \langle A\rangle^* = \mathrm{tr}\ \{A\sigma^*\}$$

$$a_o = \mathrm{tr}\ \{A\sigma_o\}$$

and the operator A is defined as:

$$A = \int_o^\infty d\tau\ \overline{[\mathcal{H}_1^*(t - \tau),\ [\mathcal{H}_1^*(t),\ Q]\ ]} \tag{2.14}$$

Substituting equation (2.9) into equation (2.14), neglecting off-diagonal terms and using for simplicity $g_{qq'}(\tau) = \delta_{qq'} g_q(\tau)$ we obtain:

$$A = \frac{1}{2} \sum_{q,p} J_q(\omega_p^{(q)})[A_p^{(q)}, [A_p^{(-q)},\ Q]\ ] \tag{2.15}$$

II.5 The Dipolar Coupling:

The complete Hamiltonian of a system of like interacting spins in a large external field may be written as:

$$\hbar\, \mathcal{H} = \hbar\ (\mathcal{H}_o + \mathcal{H}_1) \tag{2.16}$$

where the main Hamiltonian is:

$$\hbar\, \mathcal{H}_o = - \gamma\hbar H_o \sum_k I_z^k$$

The perturbing Hamiltonian $\hbar H_1$ due to the dipolar coupling is:

$$\hbar H_1 = \sum_{j<k} \frac{\hbar^2\gamma^2}{r_{jk}^3} \left\{ I^j . I^k - 3 \frac{(I^j . r_{jk})(I^k . r_{jk})}{r_{jk}^2} \right\} \tag{2.17}$$

Equation (2.17) may be written as:

$$\hbar H_1 = \frac{\gamma^2\hbar^2}{r^3} (A + B + C + D + E + F) \tag{2.18}$$

where

$$\left.\begin{aligned}
A &= I_z I_z' \, (1 - 3\cos^2\theta) \\
B &= -\frac{1}{4} (1 - 3\cos^2\theta)(I_+ I_-' + I_- I_+') \\
C &= -\frac{3}{2} \sin\theta \cos\theta \, e^{-i\phi} (I_z I_+' + I_z' I_+) \\
D &= C^* = -\frac{3}{2} \sin\theta \cos\theta \, e^{i\phi} (I_z I_-' + I_z' I_-) \\
E &= -\frac{3}{4} \sin^2\theta \, e^{-2i\phi} I_+ I_+' \\
F &= E^* = -\frac{3}{4} \sin^2\theta \, e^{2i\phi} I_- I_-'
\end{aligned}\right\} \tag{2.19}$$

Equation (2.18) can be put into the form:

$$\hbar H_1 = \sum_q F^{(q)} A^{(q)} \tag{2.20}$$

where the $F^{(q)}$ are random functions of the relative positions of the two spins and the $A^{(q)}$ are operators acting on the spin variables. We adopt the convention $F^{(q)} = F^{(-q)*}$; $A^{(q)} = A^{(-q)\dagger}$. We define

$$\left.\begin{aligned} F^{(0)} &= \frac{1 - 3\cos^2\theta}{r^3} \\ F^{(1)} &= \frac{\sin\theta\cos\theta\, e^{-i\phi}}{r^3} \\ F^{(2)} &= \frac{\sin^2\theta\, e^{-2i\phi}}{r^3} \end{aligned}\right\} \qquad (2.21)$$

and

$$\left.\begin{aligned} A^{(0)} &= \alpha\{-\frac{2}{3} I_z I_z' + \frac{1}{6}(I_+ I_-' + I_- I_+')\} \\ A^{(1)} &= \alpha\{I_z I_+' + I_+ I_z'\} \\ A^{(2)} &= \frac{1}{2}\alpha\, I_+ I_+' \qquad\qquad \alpha = -\frac{3}{2}\gamma^2 h \end{aligned}\right\} \qquad (2.22)$$

Assuming furthermore random isotropic motion for the orientation of the vector r, we have:

$$\left.\begin{aligned} \overline{F^{(q)}(t)F^{(q')*}(t + \tau)} &= \delta_{qq'}G^{(q)}(\tau) \\ J^{(q)}(\omega) &= \int_{\infty}^{\infty} G^{(q)}(\tau)e^{-i\omega\tau}d\tau \end{aligned}\right\} \qquad (2.23)$$

The equation of motion for the longitudinal magnetization will have the form:

$$\frac{d}{dt}\langle I_z + I_z'\rangle = -(a_z - a_o)$$

where $a_z = \mathrm{tr}\,\{\Lambda_z \sigma^*\}$, Λ_z being given by equation (2.15). Evaluating equation (2.15);

$$A_z = \frac{1}{2}\ J^{(1)}(\omega_I)\{[A^{(-1)},[A^{(1)},I_z + I_z']] + [A^{(-1)},[A^{(1)},I_z + I_z']]^\dagger\}$$

$$+ \frac{1}{2} J^{(2)}(2\omega_I)\{[A^{(-2)},[A^{(2)},I_z + I_z']] + [A^{(-2)},[A^{(2)},I_z + I_z']]^\dagger\} \tag{2.24}$$

Using standard commutation relations [Appendix D], we obtain:

$$[A^{(-1)},[A^{(1)},I_z + I_z']] = 2\alpha^2 I_z I_z'^2 + 2\alpha^2 I_z' I_z{}^2 - \alpha^2(I_+I_-' + I_-I_+')(I_z + I_z') \tag{2.25}$$

$$[A^{(-2)},[A^{(2)},I_z + I_z']] = \alpha^2 I_z(I_x'^2 + I_y'^2) + \alpha^2(I_x{}^2 + I_y{}^2)\ I_z' \tag{2.26}$$

Furthermore, it can be shown [Appendix D] that:

$$[A^{(-1)},[A^{(1)},\ I_z + I_z']]^\dagger = [A^{(-1)},[A^{(1)},I_z + I_z']]$$

and

$$[A^{(-2)},[A^{(2)},I_z + I_z']]^\dagger = [A^{(-2)},[A^{(2)},I_z + I_z']]$$

If we use the high temperature approximation wherein $\sigma^* - \sigma_o$ is an infinitely small quantity of the first order, quantities such as $<I_x>$, $<I_y>$, $<I_z>$ are also small of the first order and to the same approximation:

$$<I_z I_x'^2> \simeq <I_z> \frac{I(I+1)}{3}$$

$$<I_z I_z'> \simeq <I_z I_x'> \simeq 0$$

Combining equation (2.25), equation (2.26) averaging and employing the above approximation, we obtain:

$$\langle A_z \rangle \simeq \frac{2\alpha^2}{3} \, I(I+1) \, \langle I_z + I'_z \rangle \, \{ J^{(1)}(\omega_I) + J^{(2)}(2\omega_I) \} \qquad (2.27)$$

The macroscopic equation for spin-lattice relaxation then takes on the form:

$$\frac{d}{dt} \langle I_z + I'_z \rangle = - \frac{1}{T_1} \{ \langle I_z + I'_z \rangle - \langle I_z + I'_z \rangle_o \} \qquad (2.28)$$

with

$$\frac{1}{T_1} = \frac{3}{2} \, \gamma^4 \hbar^2 I(I+1) \, \{ J^{(1)}(\omega_I) + J^{(2)}(2\omega_I) \} \qquad (2.29)$$

Finally, equation (2.29) may be generalized to the case when each spin I interacts with several identical spins, provided their motions are not correlated. In such a case the equation

$$\frac{dM_z}{dt} = - \frac{1}{T_1} (M_z - M_o)$$

is still valid with:

$$\frac{1}{T_1} = \frac{3}{2} \, \gamma^4 \hbar^2 I(I+1) \, \sum_k{}' \{ J_{ik}^{(1)}(\omega_I) + J_{ik}^{(2)}(2\omega_I) \} \qquad (2.30)$$

II.6 The Spin-Lattice Relaxation Time for a Four Spin System

Assuming the four spins uncorrelated we will use equation (2.30) as the starting point.

Rewrite equation (2.21) as:

$$\left. \begin{aligned} F_{ik}^{(1)} &= \frac{\sin \theta_{ik} \cos \theta_{ik} e^{-i\phi_{ik}}}{r^3} \\ F_{ik}^{(2)} &= \frac{\sin^2 \theta_{ik} e^{-2i\phi_{ik}}}{r^3} \end{aligned} \right\} \qquad (2.31)$$

Where r is the interproton distance, θ_{ik}, ϕ_{ik} is the orientation of the H-H direction in the laboratory co-ordinate system with the magnetic field H_o along the z-axis. For a tetrahedron of protons there are six different H-H pairs. In order to evaluate the pair correlation functions we must appropriately weight the various possible orientations. At this point it is necessary to introduce a model which represents the disordered motion of the spin-carrying nuclei. To do so we introduce the reduced correlation functions

$$\tilde{g}^{(i)}(\tau) = G^{(i)}(\tau)/G^{(i)}(0)$$

and make the convenient assumption that $\tilde{g}(\tau)$ is the same for all $G^{(i)}$ and can be represented by $\exp(-|\tau|/\tau_c)$, where τ_c is a constant called the correlation time and is a characteristic of the medium.

Returning now to the weighting of the various possible orientations of the H-H pairs, it can be seen that: the probability that a pair remains at its initial orientation in a time τ is $[\frac{1}{6} + \frac{5}{6}\exp(-\tau/\tau_c)]$; and that the probability of a pair being in one of the five remaining orientations is $[\frac{1}{6} - \frac{1}{6}\exp(-\tau/\tau_c)]$. It is now possible to calculate the pair correlation functions.

Begin by considering a proton pair at orientation ij at time t. Then at time t + τ we may write:

$$F_{ij}^{(q)}(t+\tau) = [\frac{1}{6} + \frac{5}{6}\exp(-\tau/\tau_c)]\, F_{ij}^{(q)}(t) + \sum_{ik\neq ij}{}' F_{ik}^{(q)}(t)[\frac{1}{6} - \frac{1}{6}\exp(-\tau/\tau_c)] \tag{2.32}$$

Multiply equation (2.32) by $F_{ij}^{(q)}$ and also drop time independent factors, we obtain for the pair correlation function:

$$\langle F_{ij}^{(q)}(t)F_{ij}^{*(q)}(t+\tau)\rangle = \overline{\frac{5}{6}\exp(\tau/\tau_c)|F_{ij}^{(q)}|^2-\frac{1}{6}\sum_{ik\neq ij}{}' F_{ij}^{(q)}F_{ik}^{*(q)}\exp(-\tau/\tau_c)}$$

At any time, the six possible orientations are equally likely to be occupied, and therefore performing this average we obtain:

$$\langle F_{ij}^{(q)}(t)F_{ij}^{*(q)}(t+\tau)\rangle = \frac{1}{36}\exp(-\tau/\tau_c)\overline{[5\sum_{ij}|F_{ij}^{(q)}|^2-\sum_{ij}\ \sum_{ik\neq ij}{}' F_{ij}^{(q)}F_{ik}^{*(q)}]} \tag{2.33}$$

Equation (2.33) may be rewritten as:

$$\langle F_{ij}^{(q)}(t)F_{ij}^{*(q)}(t+\tau)\rangle = \frac{1}{36}\exp(-\tau/\tau_c)\overline{[6\sum_{ij}|F_{ij}^{(q)}|^2-|\sum_{ij}F_{ij}^{(q)}|^2]} \tag{2.34}$$

Taking the Fourier transform we obtain:

$$J_{ij}^{(1)}(\omega) = \frac{1}{36}\left(\frac{2\tau_c}{1+(\omega\tau_c)^2}\right)\overline{[6\sum_{ij}|F_{ij}^{(1)}|^2-|\sum_{ij}F_{ij}^{(1)}|^2]} \tag{2.35}$$

$$J_{ij}^{(2)}(2\omega) = \frac{1}{36}\ \frac{2\tau_c}{1+(2\omega\tau_c)^2}\ \overline{[6\sum_{ij}|F_{ij}^{(2)}|^2-|\sum_{ij}F_{ij}^{(2)}|^2]} \tag{2.36}$$

Finally, for a powdered sample we must average over all possible orientations of the magnetic field. Observing that $\overline{|\sum_{ij}F_{ij}^{(q)}|^2} = 0$, we then have:

$$\left.\begin{aligned}\overline{|F_{ij}^{(1)}|^2} &= \frac{2}{15}\ r^{-6}\\ \overline{|F_{ij}^{(2)}|^2} &= \frac{8}{15}\ r^{-6}\end{aligned}\right\} \tag{2.37}$$

Combining equation (2.37) with equation (2.35) and (2.36),

$$\left.\begin{aligned} J_{ij}^{(1)}(\omega) &= \frac{1}{36}\left[\frac{2\tau_c}{1+(\omega\tau_c)^2}\right][36]\,\frac{2}{15}\,\frac{1}{r^6} = \frac{4}{15}\,\frac{1}{r^6}\,\frac{\tau_c}{1+(\omega\tau_c)^2} \\ J_{ij}^{(2)}(2\omega) &= \frac{1}{36}\left[\frac{2\tau_c}{1+(2\omega\tau_c)^2}\right][36]\,\frac{8}{15}\,\frac{1}{r^6} = \frac{16}{15}\,\frac{1}{r^6}\,\frac{\tau_c}{1+(2\omega\tau_c)^2} \end{aligned}\right\} (2.38)$$

Evaluating equation (2.30),

$$\frac{1}{T_1} = \frac{3}{8}\,\gamma^4\hbar^2 I(I+1) \sum_{i\neq j}{}' \, J_{ij}^{(1)}(\omega) + J_{ij}^{(2)}(2\omega)$$

we obtain:

$$\frac{1}{T_1} = \frac{9}{10}\,\frac{\gamma^4\hbar^2}{r^6}\left[\frac{\tau_c}{1+(\omega\tau_c)^2} + \frac{4\tau_c}{1+(2\omega\tau_c)^2}\right] \qquad (2.39)$$

II.7 The Quadrupole Hamiltonian

In order to utilize the framework which has been developed thus far, the quadrupole interaction will be treated as a special case of a multipole-expansion in spherical harmonics of electrostatic energy of two charge distributions. This approach has the advantage of exhibiting clearly the various non-vanishing matrix elements of the interaction. It also yields the form of equation (2.7) with relative ease.

Consider the nucleus and the electron cloud being described by two charge distributions $\rho_n(r_n)$ and $\rho_e(r_e)$, respectively. Then their mutual electrostatic energy is given by:

$$U_E = \iint \frac{\rho_e(r_e)\rho_n(r_n)dr_e dr_n}{|\underline{r}_n - \underline{r}_e|} \tag{2.40}$$

Expanding the denominator by the classical theorem of spherical harmonics,

$$\frac{1}{|\underline{r}_n - \underline{r}_e|} = 4\pi \sum_{\ell=0}^{\infty} \sum_{m=-\ell}^{\ell} \frac{1}{2\ell+1} \frac{r_n^{\ell}}{r_e^{\ell+1}} Y_\ell^{m*}(\theta_n,\phi_n) Y_\ell^m(\theta_e,\phi_e) \tag{2.41}$$

It is assumed that $r_e > r_n$ and hence the small penetration of the electron inside the nucleus is neglected. Equation (2.40) may now be written:

$$U_E = \sum_{\ell,m} A_\ell^m B_\ell^{m*} \tag{2.42}$$

where

$$A_\ell^m = \sqrt{\frac{4\pi}{2\ell+1}} \int \rho_n(r_n)\, r_n^{\ell}\; Y_\ell^m(\theta_n,\phi_n)\, dr_n \tag{2.43}$$

and

$$B_\ell^m = \sqrt{\frac{4\pi}{2\ell+1}} \int \rho_e(r_e) r_e^{-(\ell+1)}\; Y_\ell^m(\theta_e,\phi_e)\, dr_e \tag{2.44}$$

Now if the state of the nucleus is defined by a wave function $\psi_n(R_1 \ldots R_K)$ of the co-ordinates of its K nucleons, the nuclear charge density can be written as the expectation value of the operator density of charge at the point r_n:

$$\rho_n(r_n) = (\psi_n \mid \sum_{i=1}^{K} e_i \delta(r_n - R_i) \mid \psi_n) \qquad (2.45)$$

where e_i = e for a proton and zero for a neutron. Utilizing equation (2.45), equation (2.43) may be written:

$$A_\ell^m = <A_\ell^m> \text{ where } A_\ell^m \text{ is defined as}$$

$$A_\ell^m = \sqrt{\frac{4}{2\ell+1}} \sum_i e_i R_i{}^\ell Y_\ell^m(\Theta_i, \Phi_i) \qquad (2.46)$$

where R_i, Θ_i, Φ_i are the polar co-ordinates of the K nucleons.

In a similar fashion $B_\ell^m = <B_\ell^m>$ where

$$B_\ell^m = - e \sqrt{\frac{4\pi}{2\ell+1}} \sum_{i=1}^{N} r_i^{-(\ell+1)} Y_\ell^m(\theta_i, \phi_i) \qquad (2.47)$$

where r_i, θ_i, ϕ_i are polar co-ordinates of electrons.

Consequently, the energy of the electrostatic interaction between the electrons and the nucleus is then the expectation value of the Hamiltonian:

$$H_E = \sum_{\ell,m} A_\ell^m B_\ell^{m*}$$

From equation (2.46) and (2.47) we see that the operators A_ℓ^m and B_ℓ^m transform under rotation of co-ordinate axes in the same way as spherical harmonics of order ℓ. This is the definition of tensor operators of order ℓ. The tensor operator A_ℓ with $2\ell+1$ components A_ℓ^m is called the multipole moment of order ℓ of the nucleus.

For the quadrupole moment we rewrite [Appendix E] A_2^m as:

$$\left.\begin{aligned} A_2^{\pm 2} &= \frac{\sqrt{6}}{4} \sum_i e_i (x_i \pm i y_i)^2 \\ A_2^{\pm 1} &= \frac{\sqrt{6}}{2} \sum_i e_i z_i (x_i \pm i y_i) \\ A_2^{o} &= \frac{1}{2} \sum_i e_i (3 z_i^2 - r_i^2) \end{aligned}\right\} \qquad (2.48)$$

By means of the Wigner-Eckhart theorem we may now replace $(x + iy)$ with I_+, $(x - iy)$ with I_-, z with I_z and define:

$$\left.\begin{aligned} Q^{\pm 2} &= \alpha \frac{\sqrt{6}}{4} I_\pm^2 \\ Q^{\pm 1} &= \alpha \frac{\sqrt{6}}{4} (I_z I_\pm + I_\pm I_z) \\ Q^{o} &= \alpha \frac{1}{2} (3 I_z^2 - I^2) \end{aligned}\right\} \qquad (2.49)$$

α is determined by the demand that Q^o and A^o have the same expectation value in the substate $I_z = I$; namely:

$$\begin{aligned} eQ &= (II \mid \sum_{i=1}^{K} e_i (3 z_i^2 - r_i^2) \mid II) \\ &= \alpha \, (II \mid 3 I_z^2 - I^2 \mid II) \end{aligned}$$

and finally:

$$\alpha = \frac{eQ}{I(2I - 1)}$$

We may now write equation (2.49) as:

$$\left.\begin{aligned} Q^{\pm 2} &= \frac{eQ}{I(2I-1)} \sqrt{\frac{6}{4}}\; I_{\pm}^{2} \\ Q^{\pm 1} &= \frac{eQ}{I(2I-1)} \sqrt{\frac{6}{4}}\; \{I_z I_{\pm} + I_{\pm} I_z\} \\ Q^{o} &= \frac{eQ}{I(2I-1)} \frac{1}{2} \{ 3I_z^{2} - I^{2}\} \end{aligned}\right\} \qquad (2.49a)$$

Returning to the electron operator it is seen that:

$$B_2^{o} = \frac{1}{2} \sum_{i=1}^{N} \frac{e_i(3z_i^{2} - r_i^{2})}{r_i^{5}}$$

The above is simply equal to $\frac{1}{2} \frac{\partial^2}{\partial z^2} V\Big|_{r=0}$ where $V(xyz)$ is the electrostatic potential produced by the electrons at the point x, y, z, and is still an operator. By the same argument it can be shown

$$\left.\begin{aligned} B_2^{\pm 2} &= \frac{1}{2\sqrt{6}} (V_{xx} - V_{yy} \pm 2iV_{xy}) \\ B_2^{\pm 1} &= \frac{1}{\sqrt{6}} (V_{xz} \pm iV_{yz}) \end{aligned}\right\} \qquad (2.50)$$

Combining equation (2.50) and equation (2.49a) the quadrupole Hamiltonian may be written:

$$\mathcal{H}_1 = \sum_{m=-2}^{2} A_2^{m}\mathcal{B}_2^{-m} = \sum_{m=-2}^{2} Q^{m}\mathcal{B}_2^{-m} \tag{2.51}$$

II.8 Relaxation Due to Quadrupole Coupling:

Equation (2.51) may be rewritten as:

$$\mathcal{H}_1 = \sum_{m} F^{(m)}(\Omega)A^{(m)}(I)$$

where the $F^{(m)}(\Omega)$ are lattice functions and $A^{(m)}(I)$ are spin operators, both of which transform under rotation as spherical harmonics of order 2. Ω represents the three Euler angles α, β, γ defining the orientation of the molecule with respect to the laboratory frame.

We write:

$$\left.\begin{aligned} A^{(o)}(I) &= 3I_z^{\,2} - I^2 \\ A^{(\pm 1)}(I) &= \sqrt{\frac{6}{2}}\,(I_z\, I_\pm + I_\pm\, I_z) \\ A^{(\pm 2)}(I) &= \sqrt{\frac{6}{2}}\; I_\pm^2 \end{aligned}\right\} \tag{2.52}$$

Because the unperturbed Hamiotonian $\hbar\,\mathcal{H}_o$ is $\hbar\omega_o I_z$ it follows that:

$$e^{i\mathcal{H}_o t}A^{(m)}(I)e^{-i\mathcal{H}_o t} = e^{im\omega_o t}A^{(m)}(I)$$

Also the expectation value $p^* = \mathrm{tr}(P\sigma^*)$ of any spin operator obeys the equation:

$$\frac{dp^*}{dt} = -(b^* - b_o) \tag{2.53}$$

where

$$b^* = \mathrm{tr}\{B\sigma^*\}$$

and

$$B = \frac{1}{2} \sum_m \overline{|F^{(m)}(\Omega)|^2} \; \mathcal{J}(m\omega_o)[A^{(-m)},[A^{(m)}, P]] \tag{2.54}$$

where $\mathcal{J}(\omega)$ is the Fourier transform of the reduced correlation function:

$$\mathcal{G}(t) = \frac{\overline{F^{(m)}(t)F^{(m)}(t+\tau)}}{\overline{|F^{(m)}(t)|^2}}$$

assumed to be the same for all $F^{(m)}$.

The functions $F^{(m)}(\Omega)$ can be related to the function $F^{(m)}(0)$ in the frame of the molecule by:

$$F^{(m)}(\Omega) = \sum_{m'} a_{mm'}(\Omega)F^{(m')}(0) \tag{2.55}$$

where the random character of $F^{(m)}(\Omega)$ appears in the coefficients $a_{mm'}(\Omega)$ also,

$$\overline{a_{mm'}(\Omega)a^*_{mm''}(\Omega)} = \frac{1}{2\ell + 1} \quad \delta_{m'm''}$$

where in our case $\ell = 2$, and hence we may write equation (2.54) as:

$$B = \frac{1}{10}\{\sum_{m'} |F^{(m')}(0)|^2\} \sum_m \tilde{\mathcal{J}}(m\omega_o)[A^{(-m)},[A^{(m)},P]] \tag{2.56}$$

In bulk matter there is in general, with the exception of a few paramagnetic substances such as the rare earths, no orbital degeneracy left, so the operators $\mathcal{V}_{jk}$ can be replaced by their expectation values V_{jk} taken over the single wave function representing the non-degenerate electronic state. As a consequence of this fact, the electric field gradient at the nucleus is treated classically in bulk matter and quantum-mechanically in free atoms or molecules.

Introducing the constants:

$$V^{o} = \frac{1}{2} V_{zz} = \frac{1}{2} \langle \mathcal{V}_{zz} \rangle$$

$$V^{\pm 1} = \frac{1}{\sqrt{6}} (V_{zx} \pm iV_{zy})$$

$$V^{\pm 2} = \frac{1}{2\sqrt{6}} (V_{xx} - V_{yy} \pm 2iV_{xy})$$

and hence equation (2.51) may be written:

$$\mathcal{H}_1 = \sum_m Q^m V^{-m}$$

Thus far the orientation of the Oxyz has been arbitrary. If we choose as axes of co-ordinates OXYZ the principal axes of the symmetrical tensor V_{ij} so that $V_{XZ} = V_{YZ} = V_{XY} = 0$ label these axes so that $|V_{ZZ}| > |V_{XX}| > |V_{YY}|$ and define $eq = V_{ZZ}$ and $\eta = (V_{XX} - V_{YY})/V_{ZZ}$, the quadrupole Hamiltonian becomes:

$$\mathcal{H}_1 = \frac{e^2qQ}{4I(2I-1)} \{3I_z^{\,2} - \underline{I}^2 + \frac{1}{2} \eta (I_+^{\,2} + I_-^{\,2}) \} \qquad (2.57)$$

or in terms of the $A^{(m)}$'s

$$h\,H_1 = \frac{e^2qQ}{4I(2I-1)}\,\frac{1}{h}\,\{A^{(0)} + \frac{\eta}{\sqrt{6}}\,(A^{(2)} + A^{(-2)})\,\}$$

from which

$$\left.\begin{aligned} F^{(0)}(0) &= \frac{e^2qQ}{4I(2I-1)}\,\frac{1}{h} \\ F^{(\pm 2)}(0) &= \frac{e^2qQ}{4I(2I-1)}\,\frac{\eta}{\sqrt{6}}\,\frac{1}{h} \end{aligned}\right\} \qquad (2.58)$$

Using equation (2.58) we may now evaluate equation (2.56),

$$\sum_{m'} |F^{(m)}(0)|^2 = \frac{1}{16}\left[\frac{e^2qQ}{I(2I-1)}\right]^2 [1 + \frac{\eta^2}{3}]\,\frac{1}{h^2}$$

and hence,

$$B = \frac{1}{160}\left(\frac{e^2qQ}{I(2I-1)}\right)^2 \frac{1}{h^2}\,(1 + \frac{\eta^2}{3}) \sum_m \tilde{J}(m\omega_0)\,[A^{(-m)},[A^m, P]\,] \qquad (2.59)$$

Setting $P = I_z$ and using standard commutation relations [Appendix D]:

$$\left.\begin{aligned} [A^{(-1)},[A^{(1)}, I_z]] &= \frac{3}{2}\,\{16I_z^{\,3} - I_z\,[8I(I+1) - 2]\} \\ [A^{(-2)},[A^{(2)}, I_z]] &= \frac{3}{2}\,\{-16I_z^{\,3} + I_z[16I(I+1) - 8]\} \end{aligned}\right\} \qquad (2.60)$$

Finally, carrying out the sum in equation (2.59) for the case $I = 1$ which implies $I_z^{\,3} = I_z$, we obtain:

$$B = \frac{1}{160} \left(\frac{e^2Qq}{I(2I-1)}\right)^2 (1 + \frac{n^2}{3}) \frac{1}{h^2} \{6\tilde{J}(\omega_o) + 24\, \tilde{J}(2\omega_o)\}\langle I_z\rangle$$

Recalling $\frac{dp^*}{dt} = -(b^* - b_o)$ where $b^* = tr\{B\sigma\}$ hence,

$$\frac{d}{dt}\langle I_z\rangle = -\frac{1}{T_1}\{\langle I_z\rangle - I_o\}$$

or

$$\frac{1}{T_1} = \frac{3}{80} \left(\frac{e^2qQ}{I(2I-1)}\right)^2 (1 + \frac{n^2}{3}) \frac{1}{h^2} \{\tilde{J}(\omega_o) + 4\tilde{J}(2\omega_o)\} \qquad (2.61)$$

II.9 Second Moments of N.M.R. Signals Broadened by the Dipolar Interaction (Like Spins):

We begin by recalling the dipolar Hamiltonian given by equations (2.17), (2.18), and (2.19). The use of this Hamiltonian in an attempt to calculate the shape of the absorption line in a completely general case presents an essentially impossible task. Only for a small number of interacting nuclei or for groups of nuclei displaying high symmetry is such a direct calculation feasible. However, Van Vleck (15) showed that even in the general case it is possible to calculate the moments of the line shape. If g(H) is the normalized shape function of the absorption line, then M_n the nth moment is given by:

$$M_n = \int g(H)(H - H_o)^n \, dH \qquad (2.62)$$

Of particular interest is the 2nd moment given by:

$$M_2 = \int g(H)(H - H_o)^2 \, dH \qquad (2.63)$$

The value of the 2nd moment for a single magnetic species may be written according to Van Vleck as:

$$M_2 = \frac{3}{2} I(I + 1) \gamma^2 \hbar^2 N^{-1} \sum_{j>k} \sum_{k} \frac{(3 \cos^2\theta_{jk} - 1)^2}{r_{jk}^6} \qquad (2.64)$$

where the subscripts j, k refer to the nuclear species at resonance; θ_{jk} is the angle the vector r_{jk} separating j and k makes with H_o; N is the number of nuclei at resonance.

From the standpoint of this work, a more useful formula is deduced by averaging over all orientations as for a powder sample. The angular factors become:

$$(3 \cos^2\theta_{jk} - 1)^2_{av} = \frac{4}{5}$$

so that

$$M_2 = \frac{6}{5} I(I + 1) \gamma^2 \hbar^2 N^{-1} \sum_{j>k} \sum_{k} \frac{1}{r_{jk}^6} \qquad (2.65)$$

When the nuclei at resonance are not fixed, the 2nd moment is reduced from the so called "rigid lattice" 2nd moment. To include motion the factors $(3 \cos^2\theta_{jk} - 1)^2$ appearing in the second moment must be appropriately averaged.

Let us calculate the average for a rotation about any axis. The addition theorem for spherical harmonics yields:

$$< P_\ell(\cos\theta_{jk}) >_\phi = P_\ell(\cos\theta') P_\ell(\cos\gamma_{jk}) \qquad (2.66)$$

where ϕ indicates an average over this variable.

For $\ell = 2$, we have:

$$<(3\cos^2\theta_{jk} - 1)>_\phi = \frac{1}{2}(3\cos^2\theta' - 1)(3\cos^2\gamma_{ij} - 1) \qquad (2.67)$$

The second moment for a system rotating about an axis making an angle θ' with H_o is found by substituting equation (2.67) into equation (2.64). For a powder, the axes are isotropically distributed, and since $(3\cos^2\theta' - 1)^2$ averaged over a sphere is 4/5, the 2nd moment for a powder is:

$$M_2 = \frac{1}{4}\frac{6}{5} I(I+1) N^{-1}\gamma^2\hbar^2 \sum_{j>k}\sum_k \frac{(3\cos^2\gamma_{jk} - 1)^2}{r_{jk}^6} \qquad (2.68)$$

Thus, to find the 2nd moment for a powder when the species at resonance is reorienting, one simply reduces the rigid lattice powder value by the factor:

$$F(\gamma) = \frac{1}{4}(3\cos^2\gamma_{ik} - 1)^2 \qquad (2.69)$$

If the rotational axis is normal to all internuclear vectors which contribute to the broadening then the γ_{jk} are $\pi/2$; it is then said that the 2nd moment for a powder in which such rotation occurs is one-fourth as great as if the lattice were rigid.

II.10 Line-Width Transition in a Powder Sample:

Another important problem is the rate of reorientation necessary for observation of motional narrowing. Bloembergen et al.(16) have shown that the narrowing process begins when the average period of reorientation approaches $1/2\pi\delta\nu$ where $\delta\nu$ is the line width on the frequency scale. This theory introduces a quantity ν_c, the correlation frequency, defined as $\nu_c = 1/2\pi\tau_c$, where τ_c is the correlation time. ν_c is the average rate at which significant changes occur in the atomic arrangement about a given nucleus. The motional narrowing can now be described by:

$$(\delta\nu)^2 = (\delta\nu_o)^2 \; 2/\pi \tan^{-1} \delta\nu/\nu_c \tag{2.70}$$

where $\delta\nu_o$ is the rigid lattice line width.

A physical argument describing what is happening has been given by Slichter (17). Consider the nuclei of a rigid lattice and suppose the line to have a width in angular frequency of $1/T_2^0 = \Delta\omega = \gamma\Delta H$. This line width corresponds to a spread in precession frequencies. It means that nuclei originally precessing in phase in the rigid lattice get out of step or lose their initial phase relationship in a time T_2^0. If motion of the nuclei from one point to another in the lattice occurs, a particular nucleus experiences a number of different local situations. It will sometime precess more rapidly and sometimes less rapidly. As a consequence, its mean precession frequency or integrated phase compared with the other nuclei decreases and the line therefore narrows. If this narrowing is to occur, the nucleus must necessarily sample a number of lattice sites within the time T_2^0, during which the precessions would otherwise have spread out in phase. Thus, if τ_c is a measure of the mean time the nucleus spends at a given lattice site, narrowing occurs when τ_c becomes as small as or smaller than T_2^0.

We can now find the dependence of the resulting T_2 on τ_c. Suppose there is a departure $\pm\Delta\omega$ from the mean frequency and that it lasts for a time τ_c. A phase departure $\pm\tau_c\Delta\omega$ is accumulated in this time. After n intervals, there is a mean square angular displacement $(\Delta\phi)^2 = n\ (\tau_c\Delta\omega)^2$. In time $T_2 = n\tau_c$, we say that the initial phase relationship has been lost, which we can consider to mean $(\Delta\phi)^2 \approx 1$. Thus, $1 \approx (T_2/\tau_c)(\tau_c\Delta\omega)^2$ or:

$$\frac{1}{T_2} \approx (\Delta\omega)^2\tau_c \qquad (2.71)$$

$$\tau_c < \frac{1}{\Delta\omega} = T_2^0$$

Equation (2.71) describes the course of the line narrowing as τ_c grows shorter than the T_2^0 of the rigid lattice. Equation (2.71) is basically the limiting value of equation (2.70) when τ_c is small.

A knowledge of the dependence of ν_c on temperature gives the line narrowing as a function of temperature. In the event that the reorientation is thermally activated ν_c can be expressed as:

$$\nu_c = \nu_{oc} \exp\ (-E_a/RT) \qquad (2.72)$$

where E_a is the activation energy. From the N.M.R. absorption a value of E_a can be derived by fitting equation (2.70) to the observed line width versus temperature curves. Furthermore, an estimate of the correlation frequency at the temperature where motion starts to influence the line width is obtained.

CHAPTER III

APPARATUS AND EXPERIMENTAL PROCEDURE

III.1 Introduction:

This Chapter provides a brief description of both the cw and pulse experiments including the apparatus utilized. Included also are the techniques of attaining sample temperatures higher and lower than room temperature.

III.2 Absorption Experiment:

The block diagram of the N.M.R. spectrometer is shown in Figure 1. The large magnetic field was produced by a 12" Varian electromagnet monitored by a Varian V-FR 2503 Fieldial. Two sets of pole faces with a 3" and 1½" gap produced fields of 10,000 gauss and 19,000 gauss, respectively, at maximum current. The field inhomogeneity over the samples used (9 mm in diameter by 20 mm in length) was such as to cause no significant broadening of the signals. This was checked by observing the proton signal shape of water paramagnetically contaminated by ferric nitrate. The broadening as indicated by the H_2O signal was very small compared to the natural line-widths of the signals obtained in this work.

The oscillating detector consists essentially of a marginal oscillator, a radio frequency amplifier, a detector and a wide-band audio frequency amplifier. The sample coil which is part of the resonating

Figure 1

Block diagram of the absorption spectrometer.

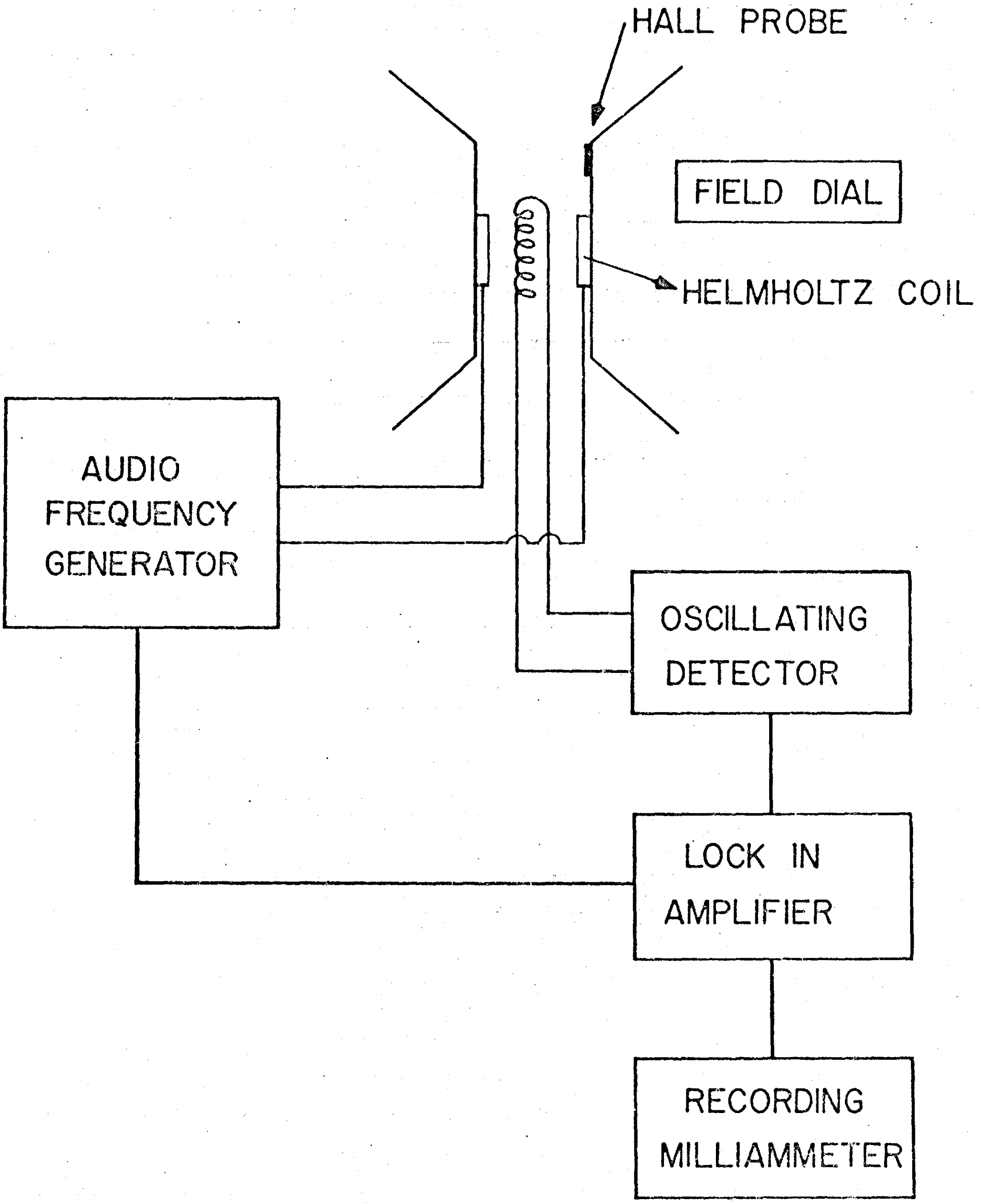
HALL PROBE
FIELD DIAL
HELMHOLTZ COIL
AUDIO FREQUENCY GENERATOR
OSCILLATING DETECTOR
LOCK IN AMPLIFIER
RECORDING MILLIAMMETER

circuit of the marginal oscillator is located in a dewar which is fixed between the pole faces of the electromagnet. A pair of Helmholtz coils are mounted on the pole faces to modulate the applied field. The frequency of the marginal oscillator is fixed. The field can be swept linearly at various rates with the help of the Fieldial. The Helmholtz coils were energized by 100 Hz alternating current supplied by a Hewlett-Packard audio frequency oscillator. The other parts of the spectrometer are a Princeton Applied Research, Model JB-4 Lock-In amplifier consisting basically of a mixer and a phase-sensitive detector, and a Hewlett-Packard 6" recording milliammeter.

The spectrometer functions as follows: the Helmholtz coils modulate the external magnetic field with an amplitude much smaller than the line-width of the N.M.R. signal. The resonance condition for the nuclei inside the sample coil, which manifests itself as a potential drop across the coil, is thus made repetitive at the modulating frequency. The signal is first r.f. amplified and detected. It is then fed to the wide-band audio-frequency amplifier followed by a lock-in amplifier, where it is mixed with the signal from the audio-oscillator and phase detected. The output of the lock-in amplifier is a d.c. signal approximately proportional to the first derivative of the absorption curve. The d.c. signal is plotted on the recording milliammeter.

With respect to the experimental conditions under which the resonances were sought, several points were borne in mind during these experiments. The density of r.f. electromagnetic energy in the sample determines the degree of nuclear spin saturation. By observing the symmetry of the shape of the resonance signals and their width as a function of r.f. power, conditions were determined under which no appreciable saturation was present. The sensitivity of the oscillating detector is greatest when the r.f. power is lowest; however, the noise level due to instabilities is greater at low r.f. power, so that power levels were used between those at which saturation or excessive noise set in. Since the signal strength depends on the number of nuclei per unit volume of the oscillator coil, maximum sensitivity was achieved by using compressed powder samples. The modulating amplitude in gauss was calibrated by observing the peak-to-peak separation of the proton signal in water as a function of modulating amplitude.

III.3 Spin-Lattice Relaxation Experiment:

The resonance condition may be approached slowly or rapidly. In the latter case, transient motions of the magnetic moment vector are set up which eventually decay to steady state motion in a time determined by the relaxation parameters T_1 and T_2.

The sample under investigation is placed in an applied magnetic field consisting of two components: a steady component of magnitude H_o oriented in the z direction and an oscillating component $2 H_1 \cos\omega t$ in the x direction. As is well known, the oscillating component can be further decomposed into two circularly polarized components in the x-y plane, rotating in opposite directions about the z-axis. Only one of these, namely, that one rotating in the same sense as the free Larmor precession of the nuclear moment, is effective in changing the orientation of the nuclear moment; the other can be ignored. The resultant moment M of the sample may be resolved into three components: M_z along the z direction, u parallel to the effective rotating component of magnetic field and v orthogonal to M_z and leading the effective rotating field component by $\pi/2$ radians. The time dependence of these three components is given by the three Bloch differential equations (18).

The transient situation may be set up by any approach to the resonance condition which is fast compared to the nutation time $1/\gamma H_1$. To do this any one of the three external parameters H_o, H_1 or ω may be varied with time in the form of a pulse starting at $t = 0$.

The pulse technique lends itself readily to a direct and straight forward measurement of the spin-lattice relaxation time T_1. Suppose that H_1 is large enough to satisfy $\gamma H_1 >> 1/T_2$, or in other words the nutation time should be short compared with the relaxation times so that the inversion of the magnetization is adiabatic. In this case the solution of the Bloch equation at resonance is:

$$M_z/M_o = m_o \exp\{-\frac{1}{2}(1/T_1 + 1/T_2)t\} [\cos\delta + (\frac{\beta-\alpha}{2}) \sin\delta] + 0(\alpha,\beta) \tag{3.1}$$

where

$M_o = \chi_o H_o$ χ_o = static susceptbility

m_o = initial value of M_z/M_o

$\delta = \gamma H_1 t$

$\beta = 1/\gamma H_1 T_2$

$\alpha = 1/\gamma H_1 T_1$

If the pulse duration is long compared with $2\, T_1 T_2/(T_1 + T_2)$, then the final value of M_z will be small compared with M_o. In other words, the sample is almost completely demagnetized. During the interval between pulses, the sample will regain some of its magnetization because of the relaxation processes. Hence, if $m_o = M_z/M_o$ is the value at the beginning of the pulse, then:

$$m_o = 1 - \exp(-t'/T_1) \qquad (3.2)$$

where t' is the time between pulses. If $m_o \lessapprox 1$, then according to the Bloch theory, v becomes proportional to m_o. Hence, by observing the dependence of the initial amplitude of v as a function of t' and making use of equation (3.2), T_1 can be directly obtained.

The experimental arrangement of the T_1 spectrometer is given in Figure 2. The spectrometer was designed by S. Vrscaj. It is capable of giving 40 gauss pulses at 11.5 MHz. The 90^o pulse length is .9 μsec in a 9 mm ID coil. The spectrometer has a fast recovery time and a high gain receiver which allows the nuclear signal to be read 6 μsec after the pulse was applied. It produces the following pulse sequences: 90^o, τ, 180^o; and 90^o, τ, 90^o, ... where τ is the pulse separation from 1 msec upward. Tektronix, series 160, pulse units were used for timing and triggering, and a Hewlett-Packard 50 MHz oscilloscope with camera was used for recording the free-induction decay amplitude.

For T_1 values above one minute, the pulse method for measuring T_1 becomes inconvenient and problems of stability tend to render the results less reliable. Fortunately, other techniques exist which lend themselves readily to the situation when T_1 becomes much longer than one minute.

The signal decay technique utilizes an experimental set-up

Figure 2

Block diagram of the T_1 spectrometer.

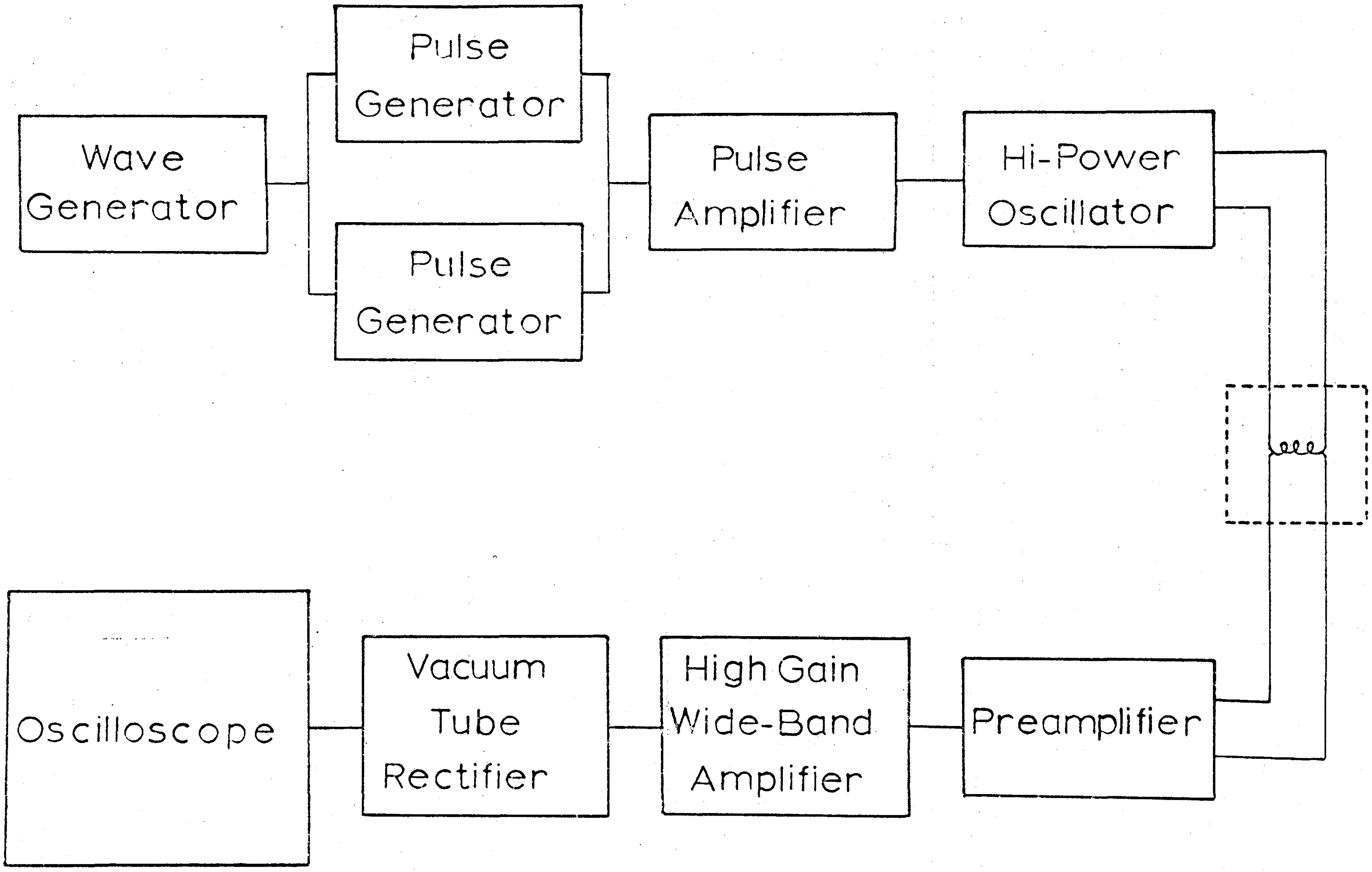
Wave Generator
Pulse Generator
Pulse Generator
Pulse Amplifier
Hi-Power Oscillator
Oscilloscope
Vacuum Tube Rectifier
High Gain Wide-Band Amplifier
Preamplifier

identical to the absorption experiment. The theory for this effect can be derived from the Bloch equations (19). The experiment proceeds as follows: The main field H_o is set on one of the peaks of the derivative curve. The r.f. power level is fixed at a definite level producing a significant amount of saturation in the absorption spectrum. The H_o field is now switched away from resonance. A time estimated to be long compared with T_1 is allowed to elapse. In our case this time was at least $4T_1$. At this time the recording milliameter is started providing a time axis, and H_o is switched back to the resonance condition. The signal is observed to decay from its value immediately after switching on H_o with a time constant which decreases, in succeeding runs, as the r.f. level is increased.

The exponentials were extrapolated to $t = 0$. All the curves intersected v_{unsat}, the amplitude of the signal in the unsaturated situation. If one defines the saturation factor S as v_{unsat}/v_{sat}, the ratio of unsaturated signal amplitude to the saturated signal amplitude, then the time constant is T_1/S.

III.4 Sample Temperature Control:

The powdered sample was encased in a thin-walled teflon cylinder. The sample coil was wound around the teflon cylinder and fixed to it by teflon tape. The sample and coil assembly were contained in a dewar which was appropriately fixed between the magnet pole faces. To obtain temperatures between 273^oK and 423^oK the boil off from liquid nitrogen was passed over a heated nichrome coil contained in a glass tube and then allowed to enter the dewar through a glass tube. Temperatures in the range from below 273°K to 85°K were achieved by nitrogen boil off without the heater. In both instances, the temperature of the sample could be controlled by varying the amount of power delivered by a variac to the immersion heater located in the liquid nitrogen source. The temperature of the sample was measured by a copper-constantan thermocouple which was buried in the middle of the sample. As a precaution against noise pick up one point of the thermocouple circuit was grounded. The thermocouple e.m.f. was measured by a Croydon Precision Instrument Co. Type P3 Potentiometer. Another thermocouple monitored the temperature of the gas outside the sample and the equality of the temperatures indicated that the sample temperature was uniform. To obtain liquid nitrogen temperature the sample dewar was filled with liquid nitrogen.

To obtain sample temperatures below 77°K a helium cooled cryogenic system was used. The dewar system and temperature controls were obtained from Andonian Associates, Inc. The sample is mounted on a copper sample holder in which are embedded two temperature sensors. In our case, the sensors are a calibrated germanium resistance thermometer and a calibrated platinum resistance thermometer. A differential copper-constantan thermocouple was used to monitor temperature gradients between sample and copper sample holder. The flow of helium gas into the sample chamber may be controlled by a needle valve connecting the pressurized helium storage chamber and sample chamber. A small electrical heater is wound on the copper sample holder. A flow of helium gas is maintained such as to yield a sample temperature slightly below that desired. Then with minimum current flow through the electrical heater, a thermal balance is obtained. This procedure minimizes the existence of temperature gradients.

After apparent temperature stabilization, a minimum of half an hour was allowed to elapse before the experiment was begun. Utilizing this procedure temperature stability could be maintained over long periods of time. At all temperatures the crystal temperature remained constant within ± 1°K for the length of time necessary to perform the experiment.

CHAPTER IV

CRYSTAL DATA

IV.1 Ammonium Sulfate:

The crystallographic data reported in 1960 by Wyckoff (20) are as follows:

Orthorhombic: space group: paraelectric phase Pnam
ferroelectric phase $Pna2_1$
Cell Dimensions: a = 7.782Å, b = 10.636Å, c = 5.993Å
Cell Contents: $4[(NH_4)_2SO_4]$ per unit cell.

The crystal belongs to the potassium sulfate structure type. The positions of the various atoms in $(NH_4)_2SO_4$ is shown in Table 1 . The crystal has three reflection planes (ab, bc, ca) and a centre of inversion. There are two inequivalent kinds of ammonium ions in the unit cell, which are denoted as Types I and II. In the ferroelectric phase, the crystal is polarized along the c axis and the centre of inversion and the ab plane of reflection are no longer present.

In Figure 3 the environment of the Type I NH_4^+ is shown above and below the transition. A comparison of Figure 3 (a) and Figure 3 (b), which show all H...O distances less than 2.6Å around one of the ammonium ions, shows that in the low-temperature phase three hydrogen atoms are

Table 1

Positional parameters above and below transition for $(NH_4)_2SO_4$

At room temperature, since the multiplicity of the general position in Pnam is eight and there are only four formula units/unit cell, the sulfur atom, two oxygen atoms, the nitrogen atoms, and four hydrogen atoms lie on the mirror planes (Positions "4c": $x, y, \frac{1}{4}$; $\bar{x}, \bar{y}, \frac{3}{4}$; $\frac{1}{2} - x, \frac{1}{2} + y, \frac{3}{4}$; $\frac{1}{2} + x, \frac{1}{2} - y, \frac{1}{4}$). The remaining atoms are in general positions (x, y, z; $\frac{1}{2} + x, \frac{1}{2} - y, \frac{1}{2} - z$; $\bar{x}, \bar{y}, \frac{1}{2} + z$; $\frac{1}{2} - x, \frac{1}{2} + y, \bar{z}$; $\bar{x}, \bar{y}, \bar{z}$; $\frac{1}{2} - x, \frac{1}{2} + y, \frac{1}{2} + z$; $x, y, \frac{1}{2} - z$; $\frac{1}{2} + x, \frac{1}{2} - y, z$). At low temperature, in Space Group $Pna2_1$ where the multiplicity of the general position is four, all atoms can occupy the general positions (x, y, z; $\bar{x}, \bar{y}, \frac{1}{2} + z$; $\frac{1}{2} - x, \frac{1}{2} + y, \frac{1}{2} + z$; $\frac{1}{2} + x, \frac{1}{2} - y, z$).

(after Schlemper and Hamilton)

		x	*y*	*z*
S	(RT)	0.244±0.001	0.419±0.001	0.250
	(LT)	0.243±0.002	0.421±0.001	0.250
	(Singh LT)	0.2421±0.0004	0.4230±0.0003	0.250
O(1)	(RT)	0.0612±0.0006	0.3887±0.0006	0.250
	(LT)	0.061±0.001	0.402±0.001	0.212±0.004
	(Singh LT)	0.0602±0.0013	0.4024±0.009	0.2127±0.0016
O(2)	(RT)	0.2701±0.0007	0.5559±0.0004	0.250
	(LT)	0.284±0.001	0.557±0.001	0.222±0.004
	(Singh LT)	0.2873±0.0015	0.5565±0.0011	0.2255±0.0018
O(3)	(RT)	0.3239±0.0005	0.3665±0.0003	0.0488±0.0005
	(LT)	0.339±0.001	0.346±0.001	0.083±0.004
	(Singh LT)	0.3375±0.0011	0.3462±0.0008	0.0872±0.0014
O(4)	(RT)	0.3239±0.0005	0.3665±0.0003	0.4512±0.0005
	(LT)	0.294±0.001	0.382±0.001	0.477±0.004
	(Singh LT)	0.2885±0.0012	0.3849±0.0009	0.4795±0.0015
N(1)	(RT)	0.6895±0.0003	0.4025±0.0002	0.250
	(LT)	0.6808±0.0007	0.3958±0.0005	0.245±0.004
	(Singh LT)	0.6789±0.0015	0.3966±0.0011	0.2533±0.0018
N(2)	(RT)	0.9677±0.0004	0.7050±0.0002	0.250
	(LT)	0.9795±0.0006	0.6999±0.0005	0.256±0.004
	(Singh LT)	0.9786±0.0014	0.7007±0.0010	0.2656±0.0016
H(1)	(RT)	0.810±0.002	0.372±0.001	0.250
	(LT)	0.771±0.003	0.336±0.002	0.202±0.005
H(2)	(RT)	0.600±0.002	0.343±0.001	0.250
	(LT)	0.564±0.003	0.360±0.002	0.206±0.005
H(3)	(RT)	0.676±0.001	0.457±0.001	0.122±0.002
	(LT)	0.691±0.002	0.480±0.001	0.157±0.005
H(4)	(RT)	0.676±0.001	0.457±0.001	0.378±0.002
	(LT)	0.682±0.002	0.412±0.002	0.408±0.005
H(5)	(RT)	1.069±0.001	0.649±0.001	0.250
	(LT)	1.092±0.002	0.658±0.002	0.222±0.005
H(6)	(RT)	0.991±0.002	0.792±0.001	0.250
	(LT)	0.990±0.003	0.793±0.002	0.265±0.008
H(7)	(RT)	0.893±0.001	0.682±0.001	0.124±0.002
	(LT)	0.896±0.003	0.670±0.002	0.142±0.005
H(8)	(RT)	0.893±0.001	0.682±0.001	0.376±0.002
	(LT)	0.945±0.003	0.672±0.002	0.412±0.005

* RT≃298°K. LT≃180°K.

Figure 3

(a) Room temperature environment of ammonium (I).

(b) Environment of ammonium (I) at approximately 180°K.

[Both (a) and (b) constitute stereoscopic pairs and can be viewed with a small hand-held stereoscope.]

(after Schlemper and Hamilton)

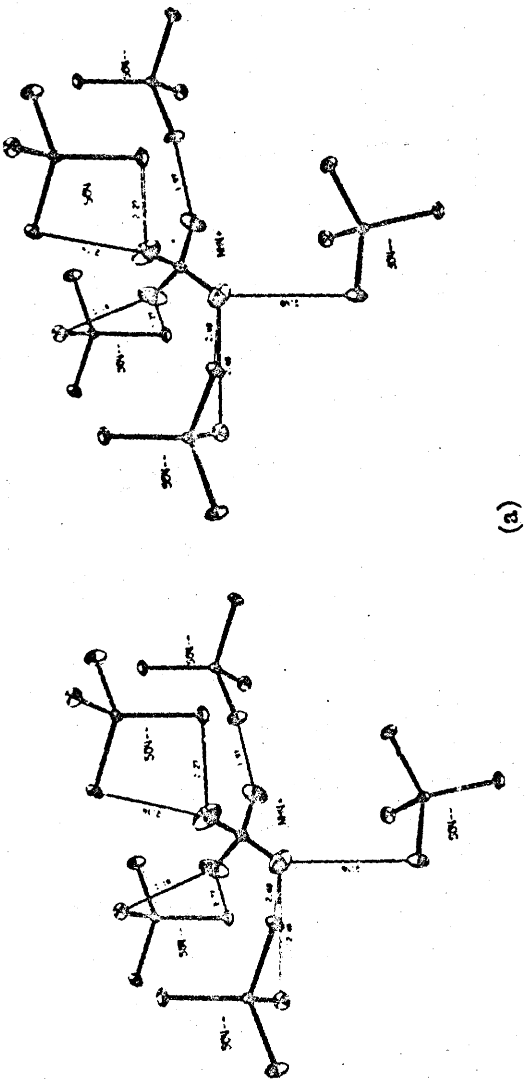

(a)

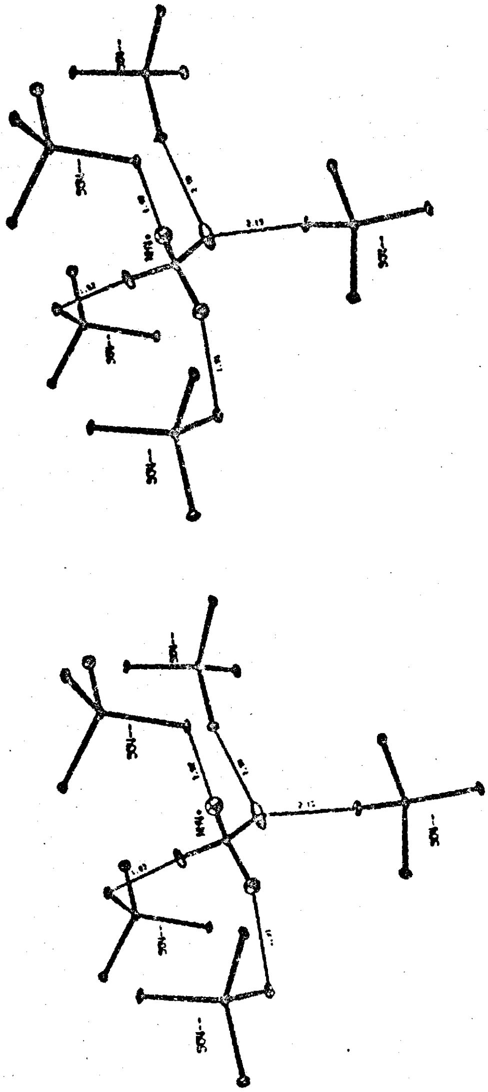

(b)

Figure 4

(a) Room temperature environment of ammonium (II).

(b) Environment of ammonium (II) at approximately 180°K.

[Both (a) and (b) constitute stereoscopic pairs and can be viewed with a small hand-held stereoscope.] (after Schlemper and Hamilton)

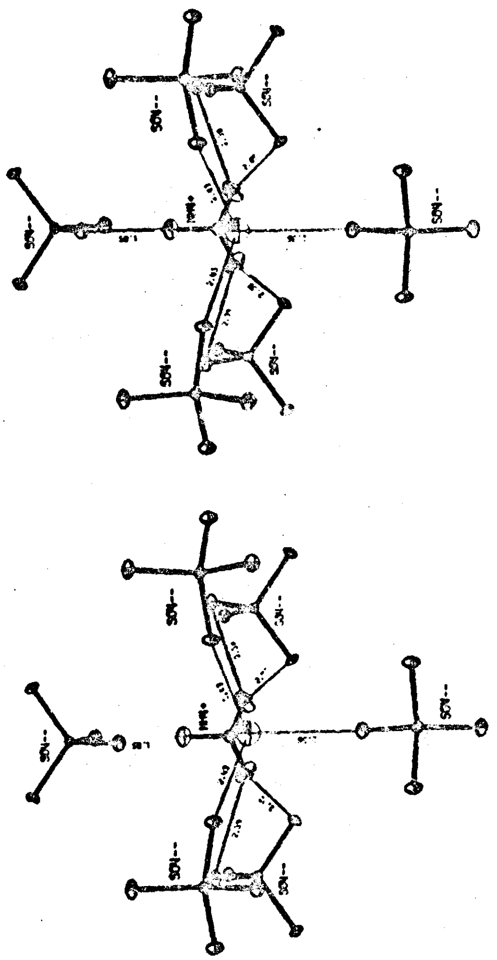

(a)

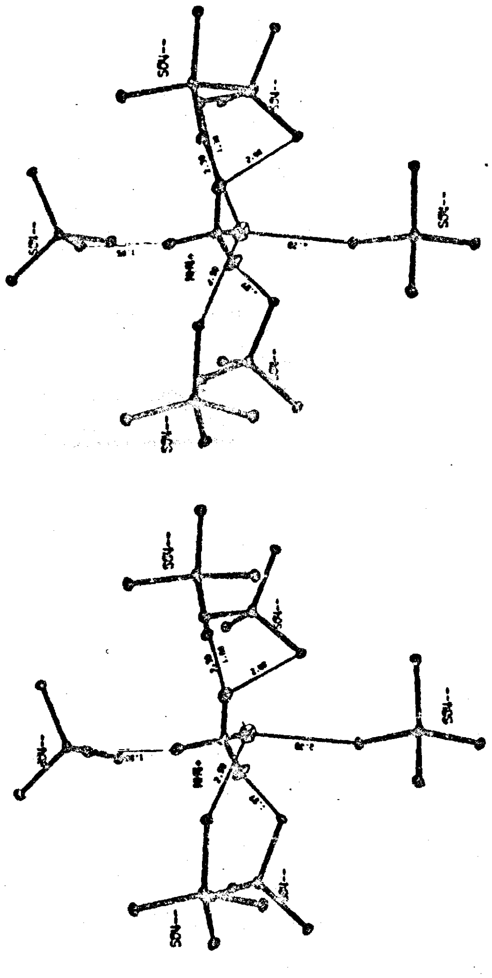

(b)

involved in strong hydrogen bonds whereas at room temperature only one hydrogen is strongly hydrogen bonded to a neighbouring sulfate group. This latter hydrogen has the weakest hydrogen bonding at low temperature. A similar comparison of Figure 4(a) and Figure 4(b) shows much less change in the hydrogen bonding around the Type II ammonium ion. However, in going from the room-temperature structure to the low-temperature structure, for that ammonium ion there is a decrease in length and presumably an increase in strength of the strongest hydrogen bond from three of the hydrogens to the neighbouring sulfates.

IV.2 Ammonium Fluoroberyllate:

The crystallographic data reported in 1960 by Wyckoff (20) are as follows:

Orthorhombic : space group; paraelectric Pnam
ferroelectric $Pn2_1a$
Cell Dimensions: a = 7.645Å, b = 10.450Å, c = 5.929Å

The crystal belongs to the K_2SO_4 structure type. The above cell dimensions are for the basic cell, but upon re-examination of the structure of $(NH_4)_2BeF_4$, Okaya et al. (21) found superstructuring with the true room-temperature cell having the b and c dimensions doubled. The symmetry of the superstructured cell of $(NH_4)_2BeF_4$ at room temperature is Acam.

Below the transition temperature $(NH_4)_2BeF_4$ has its a dimension doubled. The basic ferroelectric cell has:

$$a_f^b \simeq 2a, \quad b_f^b \simeq b, \quad c_f^b \simeq c$$

The true ferroelectric cell has a supersturcture, and

$$a_f^b \approx 2a, \; b_f \approx 2b, \; c_f \approx 2c$$

In the ferroelectric phase, the crystal is polarized along the b axis. Hence, the direction of the ferroelectric axis in $(NH_4)_2BeF_4$ is at 90° to that of $(NH_4)_2SO_4$. No information concerning the hydrogen bonding is available since detailed x-ray or neutron diffraction studies have not yet been reported.

IV.3 Sample Preparation:

The primary standard grade of ammonium sulfate was obtained from Fisher Scientific. The deuterated material was prepared by successive (three fold) isotope exchange of $(NH_4)_2SO_4$ with 99.8% D_2O.

The deuterated ammonium fluoroberyllate sample used in this study was given to us through the kindness of D. E. O'Reilly and T. Tsang.

CHAPTER V

EXPERIMENTAL RESULTS

V.1 Deuteron Spin-Lattice Relaxation in $(ND_4)_2SO_4$:

The deuteron spin-lattice relaxation times (T_1) were measured using 90° pulses at 11.5 MHz. The free-induction decay (FID) was photographed and T_1 analyzed from the amplitude of the FID following the second 90° pulse. All experimental values given in the text and in the figures are averages obtained from about 10 exposures.

The averaged experimental values of T_1 for $(ND_4)_2SO_4$ are plotted in Figure 5 on a semi-logarithmic scale versus the inverse temperature. The experiment was performed over a temperature range 475 to 105°K with data being taken at approximately 10° intervals.

The ln T_1 versus inverse temperature (1/T) relationship which describes the composite T_1 above 223°K is linear with a slope corresponding to an activation energy of 2.54 ± 0.05 kcal/mole. On passing through the first-order phase transition at 223°K, the composite T_1 decreases abruptly to about 25% of its former value.

Between the transition temperature and approximately 150°K, the decay of the magnetization was observed to be non-exponential, but could adequately be described in terms of two groups (Type I and Type II) of equal numbers of deuterons possessing different relaxation times. The

Figure 5

Temperature dependence of the deuteron spin-lattice relaxation time T_1 in $(ND_4)_2SO_4$ at 11.5 MHz.

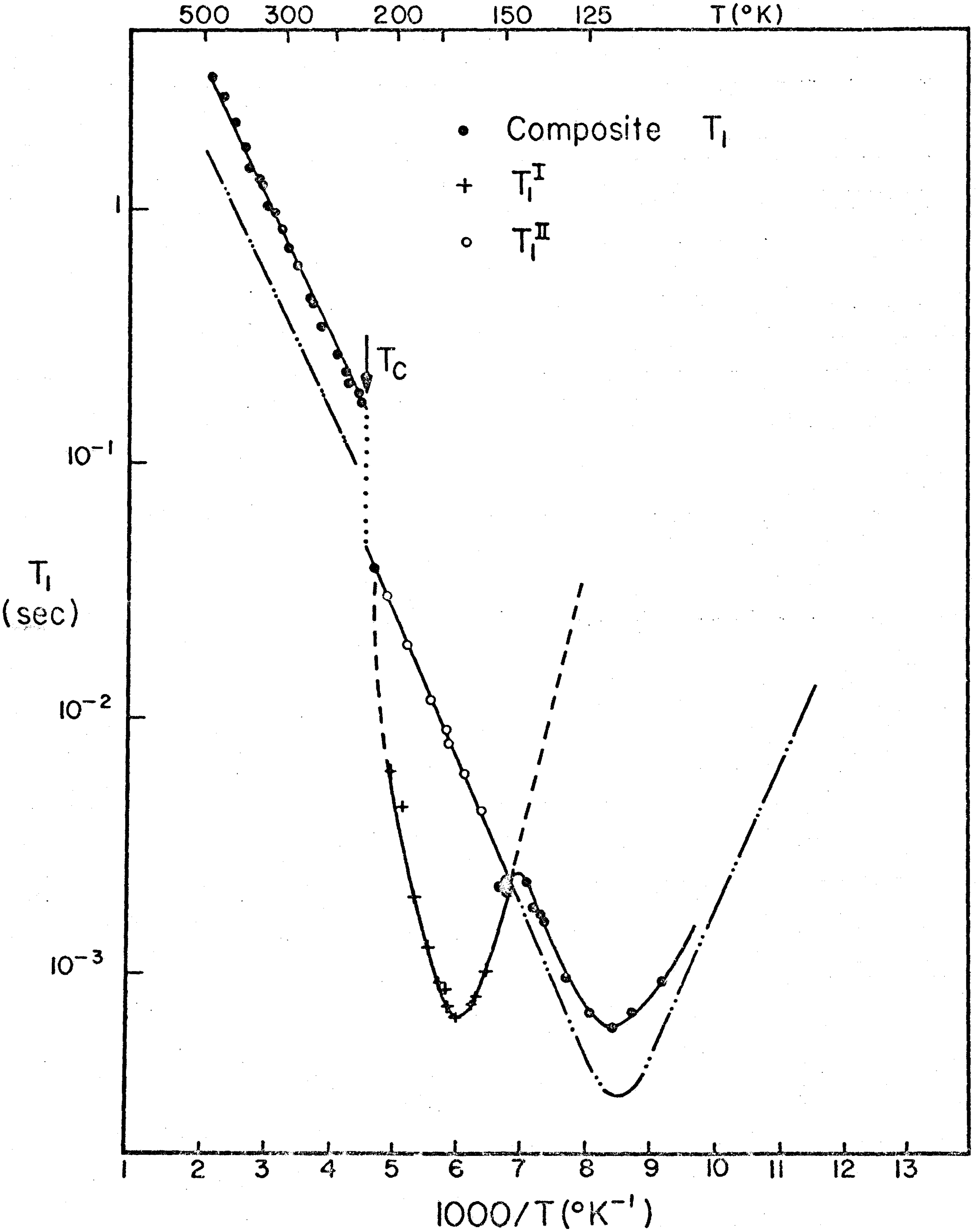
500
300
200
150
125
T(°K)
● Composite T_1
+ T_1^{I}
○ T_1^{II}
T_C
T_1 (sec)
1
10^{-1}
10^{-2}
10^{-3}
1
2
3
4
5
6
7
8
9
10
11
12
13
1000/T(°K^{-1})

experimental curve of magnetization decay in $(ND_4)_2SO_4$ at 188°K, which is typical of the observations made between 150 and 210°K, is shown in Figure 6. In this region, the ln T_1 versus 1/T relationship is not linear for Type I deuterons whereas it is linear for Type II giving an activation energy of 2.7 ± 0.3 kcal/mole. A minimum in T_1^I of 750 ± 200 μsec occurred at 165°K for Type I deuterons.

Below 150°K, the magnetization decay was again exponential indicating that the energy of both spin systems is transferred to the lattice through a single group of deuterons. After passing its minimum, T_1^I increases rapidly as the reorientation frequency of Type I deuterons decreases. Because the relaxation rate of the Type II deuterons is still increasing, this becomes the dominant relaxation mechanism and continues to be so at the lowest temperatures reached in this work. The relaxation rate of Type II deuterons reaches a maximum at 117°K producing a minimum in the composite T_1 of 630 ± 300 μsec. After the minimum, ln T_1 versus 1/T is again linear.

V.2 Deuteron Spin-Lattice Relaxation in $(ND_4)_2BeF_4$

The experimental procedure in obtaining the deuteron spin-lattice relaxation time, T_1, in $(ND_4)_2BeF_4$ was identical to that employed in the case of $(ND_4)_2SO_4$.

The averaged experimental values of T_1 for $(ND_4)_2BeF_4$ are plotted in Figure 7 on a semi-logarithmic scale versus the inverse temperature. The experiment was performed over a temperature range 475 to 77°K with data being taken at approximately 10° intervals.

Figure 6

Decay of the normalized magnetization in $(ND_4)_2SO_4$ at 188°K.

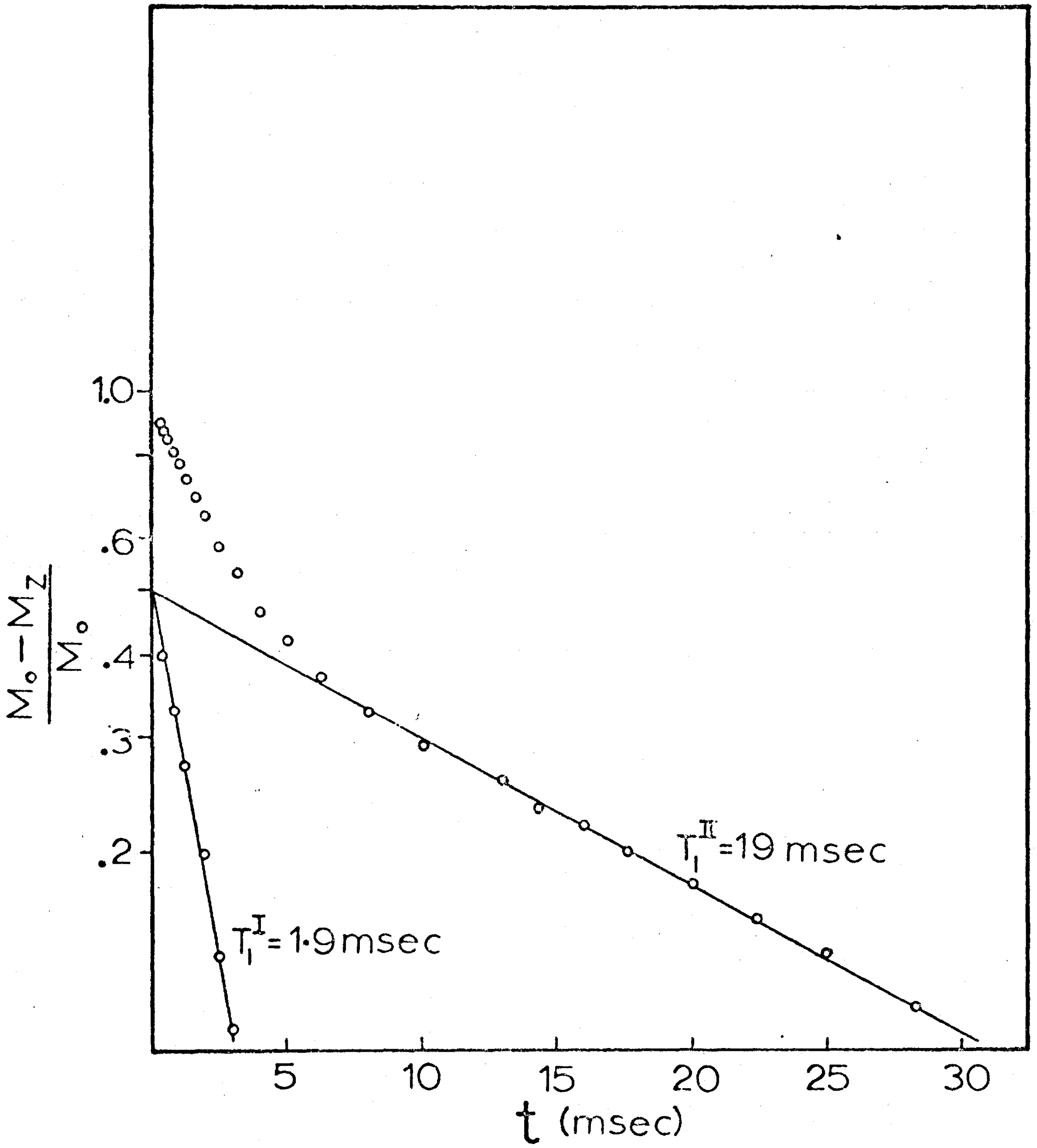
1.0
.6
.4
.3
.2
$\frac{M_o - M_Z}{M_o}$
$T_1^{II} = 19$ msec
$T_1^{I} = 1{\cdot}9$ msec
5
10
15
20
25
30
t (msec)

Figure 7

Temperature dependence of the deuteron spin-lattice relaxation time T_1 in $(ND_4)_2BeF_4$ at 11.5 MHz.

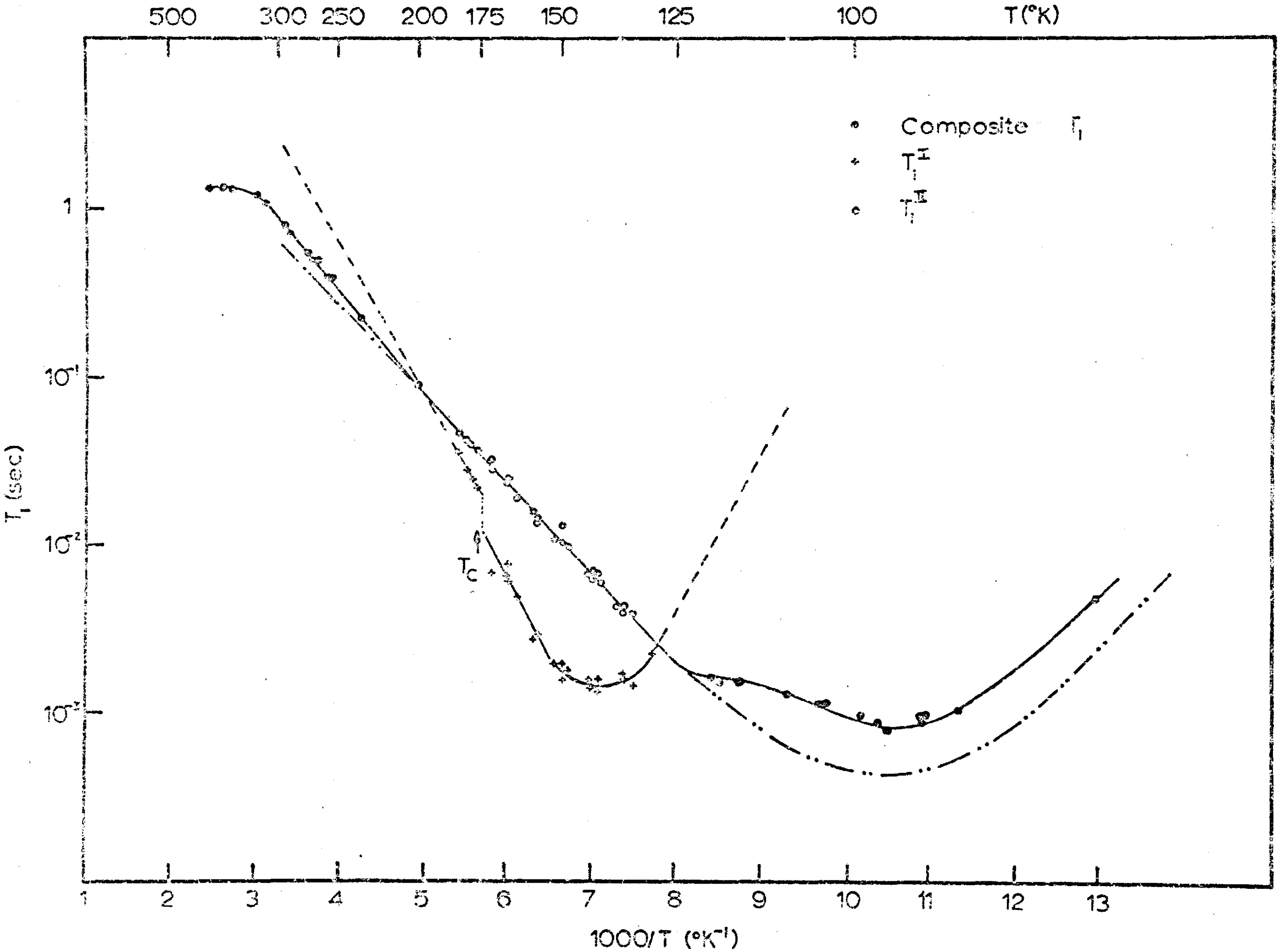
500
300
250
200
175
150
125
100
T(°K)
Composite T_1
T_1^{I}
T_1^{II}
1
10^{-1}
10^{-2}
10^{-3}
T_1 (sec)
T_c
1
2
3
4
5
6
7
8
9
10
11
12
13
1000/T (°K⁻¹)

The ln T_1 versus inverse temperature (1/T) relationship which describes the composite T_1 from 200 to 300°K is linear with a slope corresponding to an activation energy of 2.7 ± 0.3 kcal/mole. From approximately 300 to 460°K the composite T_1 increases less rapidly and the curve levels off.

Between 180 and 125°K the decay of the magnetization was observed to be non-exponential and as in the case of $(ND_4)_2SO_4$ could adequately be described in terms of two groups (Type I and Type II) of equal numbers of deuterons possessing different relaxation times. In this region, T_1^I decreases abruptly at T_c and the ln T_1 versus (1/T) relationship is linear below T_c with a slope corresponding to an activation energy of 4.3 ± 0.4 kcal/mole. On the other hand, T_1^{II} suffers no abrupt change upon passing through T_c and here also the ln T_1 versus (1/T) relationship is linear with a slope corresponding to an activation energy of 2.4 ± 0.2 kcal/mole. A minimum in T_1^I of 1500 ± 600 μsec occurred at 140°K.

Below 125°K, the magnetization decay was again exponential indicating that the energy of both spin systems is transferred to the lattice predominantly through a single group of deuterons. After passing its minimum, T_1^I increases rapidly as the reorientation frequency of Type I deuterons decreases. Because the relaxation rate of the Type II deuterons is still increasing, this becomes the dominant relaxation mechanism and continues to be so at the lowest temperatures reached in this work. The relaxation rate of Type II deuterons reaches a maximum at 95°K producing a minimum in the composite T_1 of 850 ± 300 μsec.

V.3 Proton Spin-Lattice Relaxation in $(NH_4)_2SO_4$:

Proton spin-lattice relaxation time measurements in $(NH_4)_2SO_4$ have been made at 40 MHz in a temperature range 180 to 4.2°K. The free induction technique was used in the temperature range 180 to 77°K, and, the signal decay technique in the range 77 to 4.2°K.

In Figure 8 the averaged experimental values of T_1 are plotted on a semi-logarithmic scale versus temperature in the present case, the reason being that for temperatures much below 77°K a ln T_1 versus inverse temperature plot becomes inconvenient. In the temperature region above 180°K we have included the experimental values given by Miller et al.(9). As the temperature decreases from 180°K two minima in the relaxation process are observed. The minima at 175 and 123°K correspond to the reorientation processes of the two crystallographically non-equivalent ammonium ions, Type I and Type II, respectively. The situation in the present case of proton relaxation is very similar to that observed in the deuteron relaxation experiment (see Figure 5). The difference between the two can be seen by comparing the order of magnitude of T_1 in both cases. For protons the T_1 values at both minima are at least one order of magnitude greater than those in the deuteron case. This has the result that the spin-diffusion time is shorter than both T_1^I and T_1^{II} and consequently prevents the establishment of two spin temperatures as observed for the deuterons. Therefore, in $(NH_4)_2SO_4$ both NH_4(I) and NH_4(II) ions relax through whatever group has the more effective reorientation at a particular temperature. Below 90°K, the composite T_1 begins to increase steadily and tapers off below 50°K attaining a value

Figure 8

Temperature dependence of the proton spin-lattice relaxation time T_1 in $(NH_4)_2SO_4$ at 40 MHz.

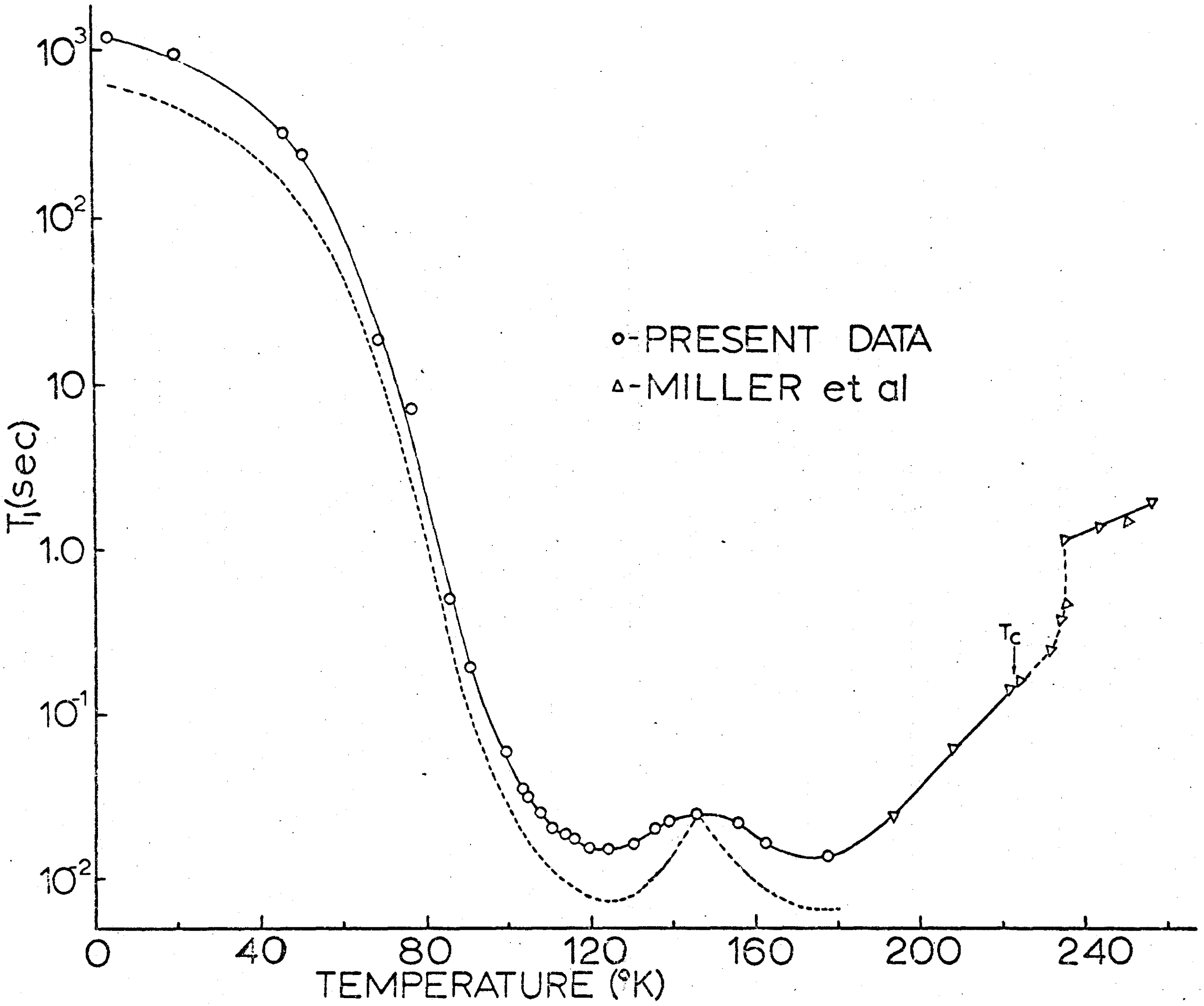
10^3
10^2
10
1.0
10^{-1}
10^{-2}
T_1(sec)
0
40
80
120
160
200
240
TEMPERATURE (°K)
○-PRESENT DATA
△-MILLER et al
T_C

of 1220 sec. at 4.2°K which is the lowest temperature reached in this experiment.

V.4 Proton Absorption Spectrum of $(NH_4)_2SO_4$:

The proton magnetic resonance absorption of $(NH_4)_2SO_4$ has been studied in the temperature region 100 to 4.2°K at 40 MHz. The present results agree with the early measurements reported by Richards and Schaefer(8).

The second moment versus temperature of the proton absorption is plotted in Figure 9. In the temperature region well above 100°K the second moment value is well below about 4 gauss^2 indicating that the intra-group local fields are almost completely averaged out. As the temperature is lowered the second moment begins to increase rapidly in the temperature range 130 to 80°K and reaches a value of 31 gauss^2 at 77°K. From 77 to 4.2°K there is no further increase in the second moment. In Figures 10 and 11 we have given sample absorption derivative curves at 105 and 4.2°K. At 105°K (Figure 10) which is in the transition region, wings begin to develop at approximately 12 gauss from the centre. At 4.2°K (Figure 11) the wings are fully developed and are situated 12 gauss from the centre.

Figure 9

Temperature dependence of the second moment of the proton absorption signal from powdered $(NH_4)_2SO_4$.

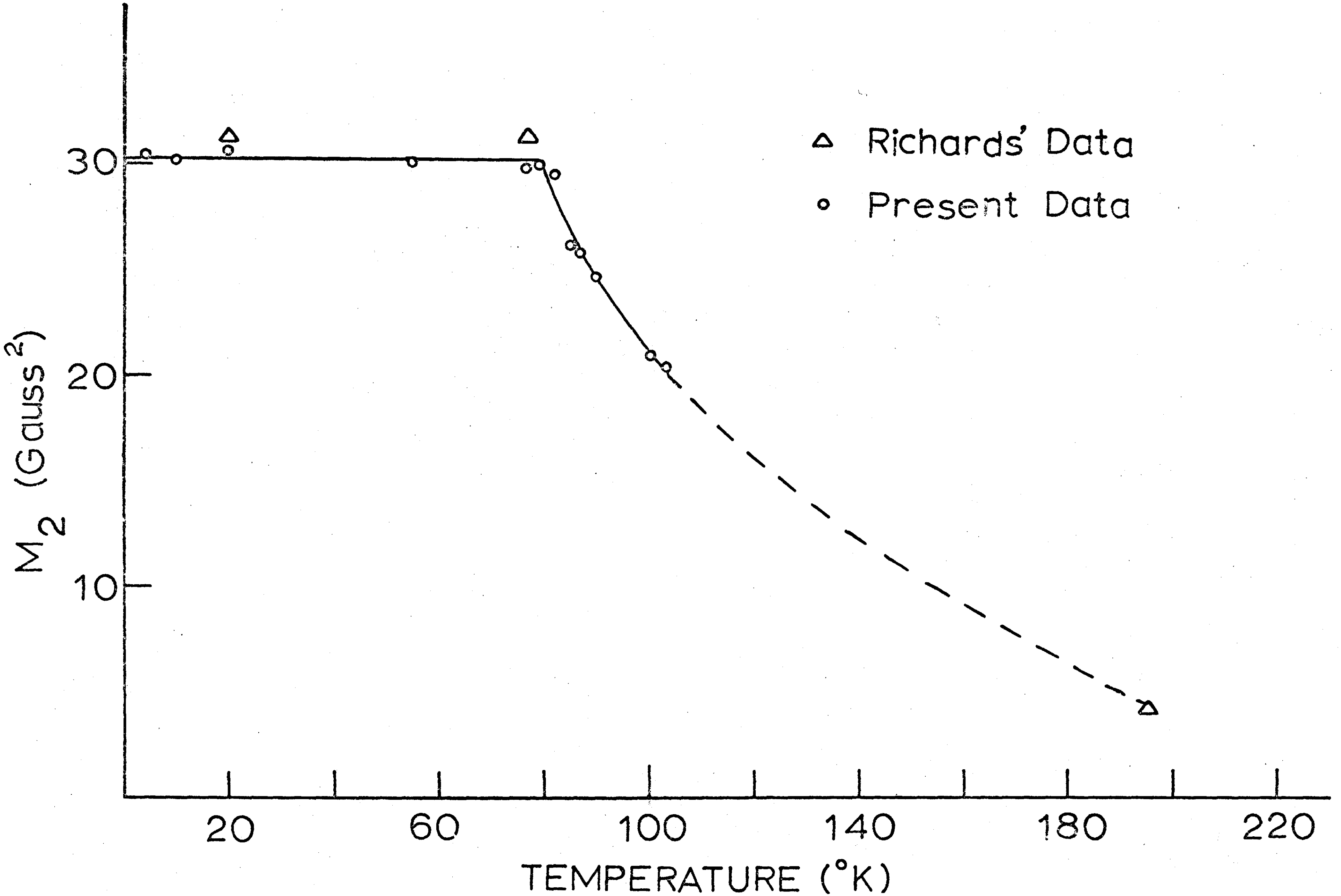
Richards' Data
Present Data
30
20
10
M_2 (Gauss^2)
20
60
100
140
180
220
TEMPERATURE (°K)

Figure 10

Proton absorption derivative curve from powdered $(NH_4)_2SO_4$ at 105°K.

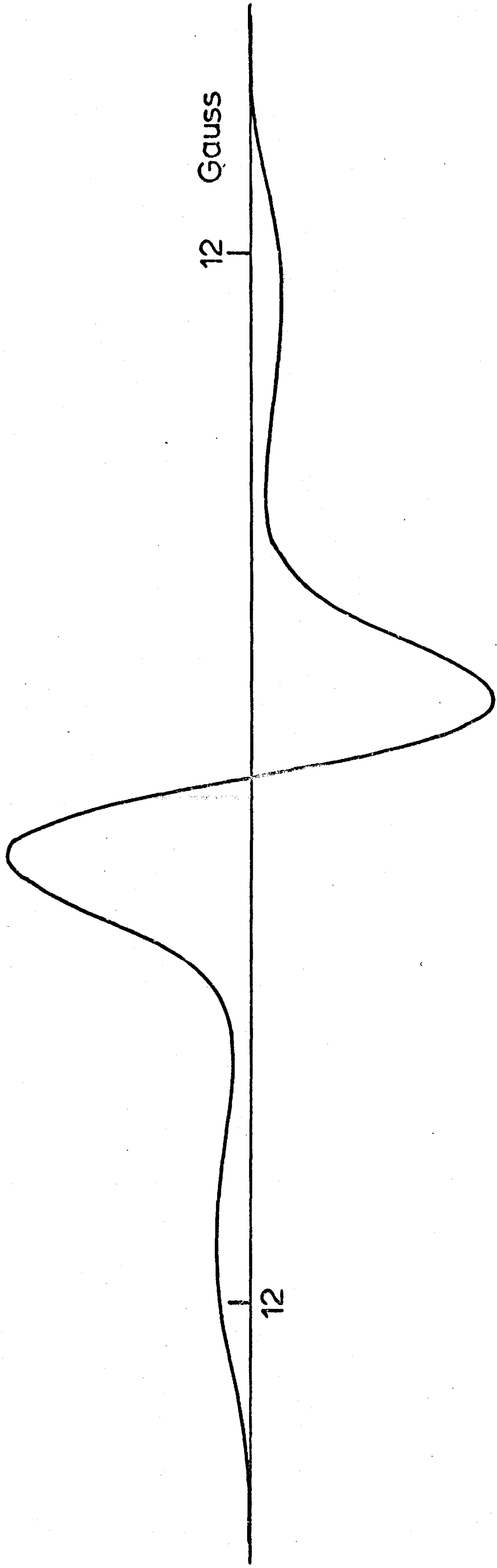
Gauss
12
12

Figure 11

Proton absorption derivative curve from powdered $(NH_4)_2SO_4$ at 4.2°K.

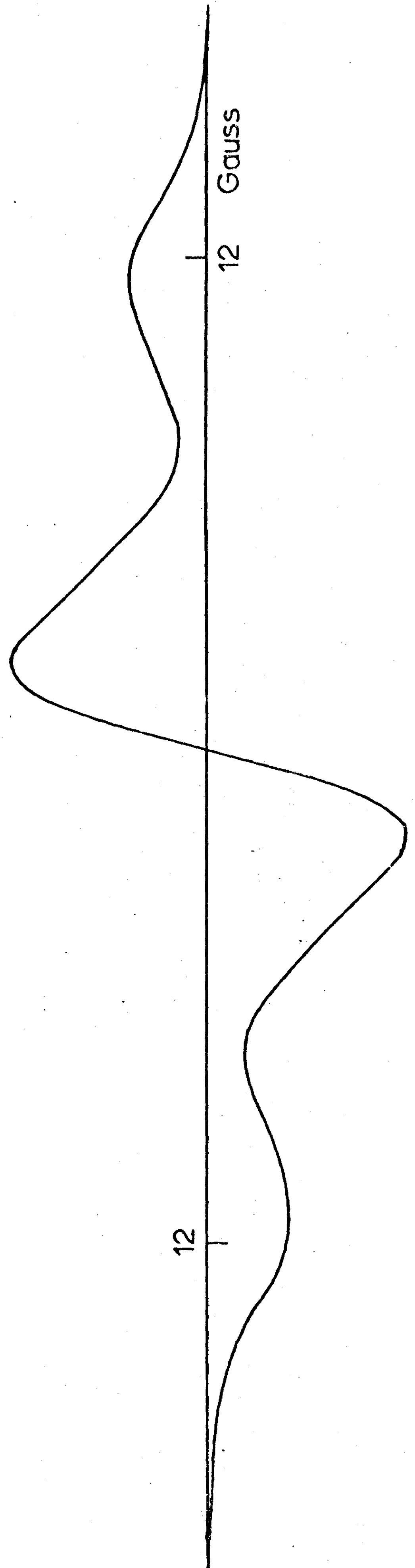
Gauss
12
12

CHAPTER VI

DISCUSSION OF EXPERIMENTAL RESULTS

VI.1 Deuteron Relaxation in $(ND_4)_2SO_4$ and $(ND_4)_2BeF_4$:

We refer to Figures 5 and 7 where the experimental values of $\ln T_1$ versus $(1/T)$ for $(ND_4)_2SO_4$ and $(ND_4)_2BeF_4$ are plotted, respectively. The temperature dependence of T_1 in each material showed a number of unusual features. The discontinuous changes in T_1 are associated with the transitions to the ferroelectric phases and, within experimental error, occurred at the reported values (3, 4) of the Curie temperatures, T_c, which are indicated in the figures.

Both ammonium sulfate and ammonium fluoro-beryllate have 8 crystallographically non-equivalent deuterons associated with two non-equivalent ND_4 groups. However, in the temperature range of interest, each ND_4 group is reorienting sufficiently fast that eqQ/h is time averaged to the same value at each of the deuteron sites within a ND_4 group but not between groups. Thus there are only two effective sub-systems of deuterons in these materials.

The two non-equivalent ammonium groups in both materials reorient against different hindering potentials and also have different quadrupolar couplings (10, 22). Consequently, the deuterons belonging to these two ammonium groups have different spin-lattice relaxation times. The observed double minima and the two values of T_1 in both materials can be understood in terms of the existence of two non-equivalent ND_4 groups in each material.

Normally, spins of the same nuclear species in a solid are more tightly coupled among themselves than with the lattice. This has the result that if the nuclei are disturbed from equilibrium with the lattice, the spin-spin interactions establish an internal equilibrium in a time less than the shortest spin-lattice relaxation time of the sub-system of spins. This situation prevents the establishment of a characteristic spin temperature for the various sub-systems of spins and as a result the nuclei act as a single system in approaching equilibrium with the lattice. The approach to equilibrium by the total magnetization, in the present case of two sub-systems of equal numbers of spins, is described by the equation:

$$M_z^{I+II}(t) = M_o^{I+II}\{1 - \exp(-t/T_1)\}$$

where M_z is the component of magnetization along the magnetic field direction, M_o is the equilibrium magnetization, and T_1 is the composite spin-lattice relaxation time given by $1/T_1 = 1/2\ (1/T_1^{I} + 1/T_1^{II})$.

However, if the spin-lattice relaxation for each of the sub-systems is faster than spin-diffusion between sub-systems, each may approach equilibrium with the lattice at a rate determined by its own T_1. Each sub-system may be said to possess its own spin temperature, θ_s, for which the rate equation for Type I in the case of two sub-systems, may be written as:

$$\frac{d}{dt}(1/\theta_s^{I}) = (1/\theta_o^{I} - 1/\theta_s^{I})/T_1^{I}$$

with an analogous one for Type II. At t=o, $\theta_o^I = \theta_o^{II}$ or, in terms of the magnetizations, M_o^I and M_o^{II}, are equal since the non-equivalent sub-systems are made up of equal numbers of deuterons. The total magnetization then approaches equilibrium at a rate determined by the characteristic time constants of the sub-systems. Again, for the case of two sub-systems of equal numbers of spins, the approach to equilibrium by the magnetization is described by the equation:

$$M_z^{I+II}(t) = M_o^{I+II} \{1 - 0.5 \exp(-t/T_1^I) - 0.5 \exp(-t/T_1^{II})\}$$

We refer to Figure 6 in which is shown the experimental curve of magnetization decay in ammonium sulfate at 188°K, which is typical of the observations made between 150 and 210°K. The experimental points represent the values of the total magnetization decay as a function of time. In order to resolve the individual time constants the longer one which in the present case is T_1^{II} is extrapolated to t = o. With the assumption that this extrapolation represents T_1^{II}, T_1^I is obtained by subtraction of T_1^{II} from the total. The applicability and limitations of this technique have been discussed by Trappaniers et al.(23). It should be noted that the extrapolated magnetization decay characterized by T_1^{II} intersects the normalized total decay at 0.5 which is what is to be expected on the assumption of two sub-systems of equal number of deuterons.

Agreement with the calculated curve using two decay constants is excellent and it is clear that in the temperature range, 150 to 210°K in $(ND_4)_2SO_4$, and, 125 to 180°K in $(ND_4)_2BeF_4$, each sub-system of deuterons approaches equilibrium with the lattice with its own relaxation time. This situation, in which both T_1^I and T_1^{II} are smaller than the spin-diffusion time, arises because the quadrupole coupling combined with molecular reorientation of both ND_4 groups produces very short values for T_1^I and T_1^{II}. Outside the temperature ranges noted above, the condition that T_1^I and T_1^{II} both be shorter than the spin-diffusion time, which is also a function of temperature, is no longer met and the magnetization decay is exponential with a single composite decay constant.

A minimum in T_1 occurs when the correlation frequencies $\omega_c^{I,II}$, of the two non-equivalent reorienting ND_4 groups satisfy the condition $\omega_L = 0.616\ \omega_c^{I,II}$ where ω_L is the deuteron Larmor precession frequency. The minimum at 165^oK in $(ND_4)_2SO_4$ occurs in the region where T_1^I and T_1^{II} can both be measured and is associated, we believe, with the deuterons denoted as Type I by Schlemper and Hamilton (12). After passing its minimum, T_1^I increases rapidly as the reorientation frequency of Type I deuterons decreases. In the region of 150^oK, T_1^I becomes larger than the spin-diffusion time between the two groups of deuterons. Because the relaxation rate of the Type II deuterons is still increasing, this becomes the dominant relaxation mechanism and continues to be so at the lowest temperatures reached in this work. The relaxation rate of Type II deuterons reaches a maximum at 117^oK producing a minimum in the observed composite T_1. In this temperature region, T_1^{II} has been calculated with the approximation that $T_1^I >> T_1^{II}$ giving $T_1^{II} = 1/2\ T_1$ except near the "crossing" temperature. Extrapolation of the T_1^I curve suggests for the region above T_c that $T_1^I >> T_1^{II}$ resulting in the Type II deuterons again providing the dominant relaxation mechanism with the composite T_1 being simply $2T_1^{II}$. If this assumption were not valid in this temperature region we would observe a larger activation energy in the paraelectric phase. It is clear from Figure 5 that the slope of T_1^{II} between 150 and 210°K is almost equal to the slope of the measured T_1 above 225°K.

The explanation for the observed behaviour of T_1 in $(ND_4)_2BeF_4$ is similar to that in $(ND_4)_2SO_4$. The minimum at 140° occurs also in the region where T_1^{I} and T_1^{II} can both be measured. In the region below 125°K Type II deuterons become the dominant relaxing mechanism. In this temperature region, T_1^{II} has been calculated with the approximation that $T_1^{I} >> T_1^{II}$ giving $T_1^{II} = 1/2\ T_1$ except near the "crossing" temperature. However, above 200°K the approximation that $T_1^{I} >> T_1^{II}$ as was the case in $(ND_4)_2SO_4$ is not valid. This may be seen by observing that the slope (see Figure 7) of the composite T_1 between about 200 and 300°K is not the same as the slope of T_1^{II} between 130 and 200°K. The reason for this lies with the values of T_1^{I} and T_1^{II} in this temperature region. In contrast to the case in $(ND_4)_2SO_4$, T_1^{I} and T_1^{II} here are comparable in value and therefore both contribute to the experimental relaxation time. The extrapolations of both T_1^{I} and T_1^{II} (see Figure 7) were obtained by using the relation $2/T_1 = 1/T_1^{I} + 1/T_1^{II}$.

The decrease of T_1 above 300°K in $(ND_4)_2BeF_4$ is probably associated with the effect of reorientation of the BeF_4 ions.

The activation energies, E_a, for the various reorientation processes have been obtained from the linear portions of the T_1 curves in Figures 5 and 7. These are compared in Table 2 with values obtained by other workers for protons in $(NH_4)_2SO_4$ and $(NH_4)_2BeF_4$. Within

Table 2

Activation energies (in kcal/mole) for reorientation of the ND_4^+ ions obtained from the T_1 data. The crystal phase for which each value was obtained is indicated in brackets after the value by the letter F or P for ferroelectric or paraelectric, respectively. Activation energies in brackets were interpreted as associated with Group I ions whereas a reinterpretation on the basis of the deuteron results show that they should be associated with Group II ions or are composite values.

	$E_a^{I}(P)$	$E_a^{I}(F)$	$E_a^{II}(P)$	$E_a^{II}(F)$	Reference
$(ND_4)_2SO_4$		5.1±1.0	2.54±0.05	2.7±0.3	
$(NH_4)_2SO_4$	(2.3±1.1)	6.1±1.2			9
	(2.3)	3.9	2.3	2.7	10
$(ND_4)_2BeF_4$	4.3±0.7	4.3±0.7	2.4±0.2	2.4±0.2	
$(NH_4)_2BeF_4$	(1.5±0.7)	5.3±1.2			9
	(2.7)	3.3		2.3	11

experimental error, the activation energies for reorientation of the Group I and II ND_4^+ ions do not change at the ferroelectric transition in agreement with the neutron results (12, 13) that the rotational freedom of the ammonium ions undergoes little change in passing through the transition.

The above results make possible an explanation for the contradictory conclusion of Miller et al. (9) that the activation energy increases substantially on going from the paraelectric to the ferroelectric phase in both ammonium sulfate and fluoroberyllate. They assumed the existence of only one effective type of ammonium ion and attributed to it the observed activation energy in each phase. In fact, their value for the activation energy in the ferroelectric phase corresponds to that of Group I ions and their value in the paraelectric phase corresponds to Group II. Interpreted on this basis, one sees that their results, shown in Table 2, are quite good within the limitations of the quoted errors.

O'Reilly and Tsang (10) and O'Reilly, Peterson and Tsang (11) did interpret their proton results in terms of two nonequivalent groups of ammonium ions, but they do not seem to have allowed for the fact that the T_1 curves for Groups I and II ions cross at two points. In the sulfate (10), the value given for Groups I and II ions in the paraelectric phase is valid only for Group II ions because these ions provide the dominant relaxation mechanism in this temperature range. In the fluoroberyllate (11), the value of 2.7 kcal/mole given for Group I ions is actually a composite value because in this range both groups of ions are effective in the relaxation process. For comparison, the deuteron results give a value of 2.7 ± 0.2 kcal/mole for the composite activation energy over the same temperature range. Fortunately, in the deuteron case, the individual activation energies for the two groups of ions can be obtained for the paraelectric phase as well as the composite value applicable at higher temperatures. This comparison shows clearly the care with which one must interpret T_1 results when dealing with crystallographically nonequivalent groups of like nuclei.

Similarly, in Table 3 our values for the correlation time, τ_{oc} at infinite temperature calculated from the condition at the T_1 minima are compared with similar values for protons.

In the case of deuterons, the dominant relaxation mechanism is expected to be quadrupolar because the magnetic moment is so small. The expression relating the quadrupole coupling constant, eqQ/h to the relaxation time is given by equation (2.61), i.e.,

$$1/T_1 = \frac{3\pi^2}{10}\ (eqQ/h)^2(1 + \eta^2/3)\left\{ \frac{\tau_c}{1 + \omega_L{}^2\tau_c{}^2} + \frac{4\tau_c}{1 + 4\omega_L{}^2\tau_c{}^2} \right\}$$

where η is the asymmetry parameter of the electric field gradients, and τ_c is the correlation time governing the exponential time decay of the auto-correlation functions for molecular reorientation. For a thermally activated reorientation, the correlation time obeys the Arrhenius relation:

$$\tau_c = \tau_{oc}\ \exp(E_a/RT)$$

From the expression for T_1 (Equation 2.61) evaluated at the extremum the quadrupole coupling constants eqQ/h can be calculated. For the Larmor frequency 11.5 MHz this expression reduces to:

$$eqQ/h = 2.6 \times 10^3\ T^{-1}_{1(min)}$$

O'Reilly and Tsang (10) have determined η in a single crystal study of $(ND_4)_2SO_4$ and found it to take for Type I and II ions respectively, the values 0.75 and 0.97 at 230°K and 0.32 and 0.52 at 210°K. The values for η are expected to continue to decrease as the temperature is lowered

Table 3

Correlation times in the ferroelectric phase.

	τ_{oc}^{I}(sec)	τ_{oc}^{II}(sec)	Reference
$(NH_4)_2SO_4$	7×10^{-14}	8×10^{-14}	10
$(ND_4)_2SO_4$	0.2×10^{-14}	10×10^{-14}	
$(NH_4)_2BeF_4$	3×10^{-14}	3×10^{-14}	11
$(ND_4)_2BeF_4$	0.2×10^{-14}	2×10^{-14}	

further and to approach zero when the ND_4 ions become rigid. Thus, the effect of η at the T_1 minima will be very small and, with the assumption that it is zero, the values shown in Table 4 were calculated for eqQ/h.

The value of 161 ± 10 kHz for eqQ/h for Type I ion in $(ND_4)_2SO_4$ compares well with the values obtained from the study of quadrupole perturbed absorption in a single crystal (10), 174 kHz, and in a powdered sample (24), 162 kHz. An eqQ/h value for Type II ion is not available for comparison because these ions are reorienting too fast at the lowest temperature reached in the quadrupole perturbed absorption experiment. No data in the case of $(ND_4)_2BeF_4$ are available for comparison.

In conclusion it is interesting to compare the present results with those obtained from other experiments. The observation of distinctly different relaxation times for the two non-equivalent groups of deuterons in both materials confirms the interpretation given by O'Reilly and Tsang (10,11) for the occurrence in the ferroelectric phase of two minima in the temperature dependence of the proton relaxation time. The values obtained for the activation energy of the Type II deuterons over different temperature ranges in the case of $(ND_4)_2SO_4$ are the same (within experimental error) in agreement with the conclusion drawn from neutron diffraction work (12, 13) that no significant change in the activation energy takes place at the ferroelectric transition. In this respect, the deuteron results are clearer than the proton results (10) where the direct measurement of the activation energy appears to be for Type II protons above the transition and Type I below.

Table 4

Quadrupole coupling constants eqQ/h in kHz.

	Type (I) Ion	Type (II) Ion
$(ND_4)_2SO_4$	161 ± 10	232 ± 18
$(ND_4)_2BeF_4$	107 ± 8	200 ± 14

[illegible]

O'Reilly and Tsang (10) have proposed a model for the ferroelectric transition in both materials based on their deuteron magnetic absorption results. They suggest that the transition from the paraelectric to the ferroelectric phase is due to the tilting of the distorted ammonium tetrahedra along the respective ferroelectric axes. Based on this model, calculations of the spontaneous polarization in both materials, and of the latent heat in ammonium sulfate, are in good agreement with the experimental data (5).

It is interesting to compare the effects of the ferroelectric phase change on T_1 in ammonium sulfate and ammonium fluoroberyllate in the light of the present deuteron spin-lattice relaxation results where we are able to resolve the individual correlations of the two independent ammonium groups. In Figure 7, it is clear that in ammonium fluoroberyllate only one ammonium group (Type I) suffers discontinuous change in T_1 at T_c. From a comparison of Figures 5 and 8 showing the deuteron and proton relaxation results, respectively, it is evident that in ammonium sulfate both ammonium groups suffer a discontinuous change in T_1 at T_c.

The above suggests that the phase transitions in these two materials are rather different and that in ammonium sulfate both types of ammonium ions are involved whereas in ammonium fluoroberyllate only one type is involved. Such a conclusion is supported by thermal and dielectric results (5). From these thermal studies, the entropy change at the transition was found to be 1.90 cal/mole deg. for $(NH_4)_2BeF_4$ and 2.27 cal/mole deg. for $(ND_4)_2BeF_4$ compared to almost twice as large a value, 4.2 cal/mole deg., observed for $(NH_4)_2SO_4$ and $(ND_4)_2SO_4$. The dielectric results are of particular interest if the ammonium ions do indeed make the major contribution to the spontaneous polarization but they are difficult to compare because of their different temperature dependences. In $(NH_4)_2BeF_4$ the spontaneous polarization, after a rapid initial increase at the phase transition, continued to increase slowly as the temperature was lowered whereas it showed no temperature dependence after the initial large increase at the transition in $(NH_4)_2SO_4$. Nevertheless, the spontaneous polarization reached a value of only 0.22 μcoul/cm^2 at 153^{o}K in the fluoroberyllate compared to 0.47 μcoul/cm^2 in the sulfate.

It also is interesting to note that for the N.M.R. results the phase transition in ammonium fluoroberyllate appears to be first order and just as abrupt as in ammonium sulfate. This is supported by a more recent dielectric study of the fluoroberyllate the results of which indicate that the transition is first order (6).

VI.2 Low Temperature Proton Magnetic Resonance in $(NH_4)_2SO_4$:

Although there exist data in the literature for proton absorption in $(NH_4)_2SO_4$ down to 20^{o}K, we repeated the experiment from 100 to 20^{o}K and extended it down to 4.2^{o}K. The temperature dependence of the second moment is given in Figure 9. The agreement with earlier results (8) is generally good, although the value of the second moment at 4.2^{o}K is approximately 10% smaller than that reported at 20^{o}K. The experimental value of 31 gauss^2 for the second moment at 4.2^{o}K is significantly lower than reported values for similar proton configurations. For example, in NH_4Cl, NH_4NO_3, NH_4IO_3 and $(NH_4)_2CrO_4$, the second moment at 20^{o}K is approximately 50 gauss^2 (8).

According to a theoretical calculation (26) a rigid tetrahedral four-proton spin configuration with proton-proton distance approprate for the NH_4 group, would be expected to produce a second moment of about 50 gauss^2. The observed value in $(NH_4)_2SO_4$ which is about 40% lower indicates that some phenomenon is preventing the rigid lattice value from being attained. It should be mentioned that this unusual narrow line-width is not isolated to the present case of $(NH_4)_2SO_4$. Significant narrowing of the proton second moment at liquid helium temperature has been observed in this laboratory for about ten ammonium compounds, and, a very similar reduction has been reported for solid methane (27). As a result of these observations, it is evident that the reduction in line-width, whatever its nature, appears to occur often with tetrahedral configurations of nuclei with $I = 1/2$.

To differentiate between a motional narrowing, where the correlation frequency is larger or equal to the line-width, and a narrowing due to symmetry selection rules imposed on the total wave function, spin-lattice relaxation times were measured at 40 MHz down to 4.2^{o}K. The present T_1 results indicate that the correlation frequency is indeed much smaller than the line-width with the consequence that motional narrowing is not taking place in $(NH_4)_2SO_4$ at 4.2^{o}K.

The low temperature T_1 data to which we refer are given in Figure 8. We observe that below 90^{o}K, T_1 begins to increase steadily and then tapers off below 50^{o}K attaining a value of 1220 sec at 4.2^{o}K. This temperature dependence suggesting a limitation of T_1 usually suggests that the effective relaxation mechanism is due to paramagnetic impurities.

The argument which leads to the conclusion that motional narrowing, as for example due to thermally activated reorientation or tunneling, is incapable of line narrowing in $(NH_4)_2SO_4$, proceeds as follows: The dipolar relaxation rate for a four-spin system is given by equation (2.39), i.e.

$$\frac{1}{T_1} = \frac{9}{10}\frac{\gamma^4 \hbar^2}{r^6} \left\{ \frac{\tau_c}{1+\omega_L^2\tau_c^2} + \frac{4\tau_c}{1+4\omega_L^2\tau_c^2} \right\}$$

Using the approximation that at the low temperature side of the T_1 minimum $\omega_L\tau_c >> 1$, equation (2.39) reduces to:

$$T_1 = \frac{5}{9}\frac{r^6}{\gamma^4 \hbar^2}\frac{\omega_L^2}{\tau_c}$$

This frequency dependence was checked at 25 and 40 MHz in the region of 70°K and found to hold within experimental accuracy. Assuming that the experimental value of 1220 sec for T_1 at 4.2°K represents a purely dipolar relaxation rate we calculate ω_c (motion) = 2π (200)$\sec^{-1}$. This value is two orders of magnitude smaller than the line-width of the NH_4 group ($\sim 10^5$ Hz) at 4.2°K. Consequently, the possibility of motional narrowing is ruled out.

As mentioned prevously, the temperature dependence of the observed T_1 in the region 50 to 4.2°K suggests a paramagnetic impurity relaxation mechanism. In the event that paramagnetic impurity relaxation contributes to the observed rate we may write:

$$\left(\frac{1}{T_1}\right)_{\text{experimental}} = \left(\frac{1}{T_1}\right)_{\text{dipolar}} + \left(\frac{1}{T_1}\right)_{\text{paramagnetic}}$$

As a result, the dipolar rate will be smaller than the one observed and hence equation (2.39) becomes an inequality yielding ω_c (motion) $\leqq 2\pi$ (200) $\sec^{-1}$. It is clear that this observation reinforces our conclusion that motion in incapable of averaging out the local field.

To be complete we should discuss the possibility that one of the two non-equivalent NH_4 groups is motionally affected while the other is at rest. In this case $1/T_{1\ \mathrm{exp}} = 1/2\ (1/T_1^I + 1/T_1^{II})$ and since one rate is zero we are left with T_1^I (or T_1^{II}) $= 1/2\ T_{1\ \mathrm{exp}}$ which will increase the correlation frequency by a factor of two. It then follows that ω_c (motion) $\leqq 2\pi$ (400)$\sec^{-1}$ which is still well below the line-width and hence further strengthens our argument that motion is incapable of averaging out the local field.

Having ruled out motional mechanisms as possible causes for the observed line narrowing, a possible explanation of the narrowing could be the symmetry requirement that the total wave function be symmetric under the exchange of two pairs of protons. This symmetry requirement imposes selection rules on the spatial and spin wave functions and restricts the possible combinations of rotational and the total nuclear spin quantum numbers.

It is known (14 - pg. 106) that terms in the dipolar Hamiltonian which couple states of different energy must be dropped in the calculation of the second moment, since their contribution contains factors which oscillate very rapidly and consequently average out. This is the reason why only terms A and B of the dipolar Hamiltonian [equation (2.19)] are retained in the second moment calculation, since only these terms involve $\Delta M = 0$ (i.e. $\Delta E = 0$). It should be pointed out that the inclusion of the terms C, D, E, F, of the dipolar Hamiltonian introduces matrix elements in the Hamiltonian function of the type $\Delta M = \pm 1, \pm 2$. As a result transitions are now allowed at energies of $2\hbar\omega_L$, and 0, which are not observed because they are shifted away from the Larmor frequency. It should be mentioned that the dropping of these non-adiabatic terms is not just a simplification but necessary if we are to use the departure of the mean square frequency from $(\hbar\omega_L)^2$ as a measure of the mean square line-width of the main line. The subsidiary lines are much fainter than the primary Larmor component, but differ so much from the latter in frequency that their contribution to the mean square frequency deviation is of the same order as the mean square width of the dominant line.

Returning now to the situation where the spin and rotational states are not considered in dependently, then their combinations are governed by symmetry requirements. For the case of four protons on the corners of a tetrahedron the total spin quantum number I of the molecule combines with the rotational angular momentum quantum numbers, L, such that, for example, I = 2 spin states only combine with even L rotational states. This is a necessary consequency of the anti-symmetry of the total wave function ψ under exchange of two protons (fermions), or in other words, ψ is symmetric under any real rotation of the tetrahedron.

Under these circumstances, the terms A and B of the dipolar Hamiltonian have non-zero matrix elements between states of different I, and hence of different L. Since states of different L have different energies these transitions will be shifted in frequency and consequently will not be observed. Therefore, these matrix elements must be dropped from the calculation of the second moment, resulting consequently in a lowering of the second moment.

Quantitative estimates based on this possible narrowing mechanism are not available at present. Since this effect is not peculiar to $(NH_4)_2SO_4$, but appears to occur reasonably often with tetrahedral configurations of nuclei with $I = 1/2$, an effort is presently being made in this laboratory to help resolve this problem.

APPENDIX A

CORRELATION FUNCTIONS

Consider a function $y(t)$ where t refers to time. $y(t)$ is a random function if the value y which it takes at each t is a random variable subject to a law of probability $p(y,t)$.

The average value of $y(t)$ is:

$$\overline{y(t)} = \int y\ p(y,t)\ dy \tag{A-1}$$

Also if $f(y)$ is a given function of y, f will also be a random function of t and:

$$\overline{f(t)} = \int p(y,t)\ f(y)\ dy \tag{A-2}$$

We define the function $p(y_1t_1;\ y_2t_2)$ as the probability of y taking on a value y_1 at t_1 and y_2 at t_2. A function having a slightly different meaning and which is represented by $P(y_1,t_1;\ y_2t_2)$ is the probability that y takes on the value y_2 at t_2 when we know that it takes the value y_1 at t_1. Hence, we may write:

$$p(y_2,t_1;\ y_1,t_1) = P(y_1t_1;\ y_2t_2)\ p\ (y_1,\ t_1) \tag{A-3}$$

The auto-correlation function $G(t_1,t_2)$ of the random function $f(y)$ relative to the times t_1 and t_2 is defined:

$$G(t_1,t_2) = \overline{f(t_1)f^*(t_2)} = \iint p(y_1,t_1,y_2,t_2)f(y_1)f^*(y_2)dy_1dy_2$$

$$G(t_1,t_2) = \iint p(y_1,t_1)\ P(y_1t_1;y_2t_2)f(y_1)f^*(y_2)dy_1dy_2 \qquad \text{(A-4)}$$

We are interested in a class of random functions which are invariant under change of origin of time and are called stationary random functions. For this class $p(y,t)$ is in fact time-independent and $p(y_1t_1,y_2t_2)$, $P(y_1t_1,y_2t_2)$ and $G(t_1t_2)$ depend on t_1 and t_2 only through the difference $t_2 - t_1 = \tau$. Or:

$$G(\tau) = \iint p(y_1,y_2,\tau)\ f(y_1)\ f^*(y_2)\ dy_1dy_2$$

$$G(\tau) = \iint p(y_1)\ P(y_1y_2,\tau)\ f(y_1)\ f^*(y_2)\ dy_1dy_2 \qquad \text{(A-5)}$$

We define a correlation time τ_c by the condition that $G(\tau)$ is very small for $|\tau| >> \tau_c$.

We also have the property that:

$$p(y_1y_2,\tau) = p(y_2,y_1, -\tau)$$

and according to equation (A-5) we may write:

$$G(-\tau) = G^*(\tau) \qquad \text{(A-6)}$$

If we assume symmetry between past and future so that:

$$p(y_1y_2\ -\tau) = p(y_1y_2\tau)$$

we obtain:

$$G(-\tau) \;=\; G^{*}(\tau) \;=\; G(\tau) \qquad \text{(A-7)}$$

The auto-correlation function is both an even and a real function of τ.

Finally, we introduce the Fourier transforms of G.

$$\begin{aligned} j(\omega) &= \int_{0}^{\infty} G(\tau)\; e^{-i\omega\tau} d\tau \\ J(\omega) &= 2\int_{0}^{\infty} G(\tau)\; \cos(\omega\tau)\; d\tau \;=\; \int_{\infty}^{\infty} G(\tau)\; e^{-i\omega\tau} d\tau \qquad \text{(A-8)} \\ k(\omega) &= \int_{0}^{\infty} G(\tau)\; \sin(\omega\tau)\; d\tau \end{aligned}$$

from which we have:

$$j(\omega) \;=\; \frac{1}{2}\; J(\omega) \;-\; ik(\omega) \qquad \text{(A-9)}$$

APPENDIX B

B.1 Properties of the Density Matrix:

The expectation value of an operator Q over the wave function $\psi(xyzt)$ is:

$$\langle Q \rangle = \langle \psi \mid Q \mid \psi \rangle \tag{B-1}$$

$\psi(xyzt)$ may be expanded in terms of an orthonormal set $(\phi_1(xyz), \phi_2 \cdots)$ as:

$$\psi(xyzt) = \sum_k C_k(t)\, \phi_k(xyz) \tag{B-2}$$

If we now substitute equation (B-2) into equation (B-1)

$$\langle Q \rangle = \sum_{i,k} C_i^*(t) C_k(t) \langle \phi_i \mid Q \mid \phi_k \rangle \tag{B-3}$$

The above represents the average value of Q over the range of possibilities presented by each member of an ensemble of systems. What corresponds, however, to an actual measurement on the physical system is an average over all systems of the ensemble. Hence, we are interested in:

$$\overline{\langle Q \rangle}^{\text{ensemble}} = \sum_{i,k} \overline{C_i^*(t) C_k(t)}^{\text{ensemble}} \langle \phi_i \mid Q \mid \phi_k \rangle$$

where

$$\overline{C_i^*(t) C_k(t)}^{\text{ensemble}} = \frac{1}{N} \sum_{\alpha=1}^{N} C_{i\alpha}^*(t) C_{k\alpha}(t)$$

for N systems $\alpha = 1, 2, \ldots N$ of an ensemble.

We define the density matrix ρ_{ki} as:

$$\rho_{ki} = \overline{C_i^*(t)C_k(t)}^{\text{ensemble}} \tag{B-4}$$

Finally,

$$< Q > = \sum_{i,k} \rho_{ki} Q_{ik} = \mathrm{tr}(\rho Q) \tag{B-5}$$

where

$$Q_{ik} = <\phi_i \mid Q \mid \phi_k>$$

B.2 The Density Matrix as an Operator:

Thus far ρ has been defined using a particular basis. Changing the basis changes the form of the density matrix in the usual way. Suppose $(\phi_1 \phi_2 \ldots \phi_n)$ are the first basis and that $(\chi_1 \chi_2 \ldots \chi_n)$ are a new set related by the transformation $(\chi_1 \chi_2 \ldots \chi_n) = (\phi_1 \phi_2 \ldots \phi_n)U$ where U is an nxn matrix of coefficients. Then ρ^χ, the density matrix in the χ representation is related to ρ^ϕ by:

$$\rho^\chi = U^{-1} \rho^\phi U \tag{B-6}$$

As ρ^χ and ρ^ϕ describe the same system, although they look quite different, it is more desirable to define a density matrix operator $\overset{=}{\rho}$, from which a matrix can be formed with any basis in the usual way.

$$\rho^\phi_{ij} = \int \phi_i \, \overset{=}{\rho} \, \phi_j d\tau$$

To do this recall:

$$<\phi_i \mid \phi_j> = \int \phi_i^* \phi_j \, d\tau$$

and

$$<\phi_i \mid Q \mid \phi_j> = \int \phi_i^* Q \phi_j \, d\tau = Q_{ij}$$

Hence, with the basis $(\phi_1 \phi_2 \ldots)$

$$\rho_{ij} = < \phi_i \mid \bar{\bar{\rho}} \mid \phi_j >$$

If we choose the basis $(\chi_1 \chi_2 \ldots)$ where $\bar{\bar{\rho}}$ is diagonal the only elements are diagonal such as ρ_{ii}^{χ}. The operator

$$\bar{\bar{\rho}} = \sum_i \mid \chi_i > P_i < \chi_i \mid \qquad \text{(B-7)}$$

where the P_i are numbers, also only has diagonal elements $\rho_i^{\chi} = P_i$. This is the density matrix operator and from it the density matrix can be written in any basis, e.g., in the ϕ basis.

$$\rho_{ij}^{\phi} = \sum_k < \phi_i \mid \chi_k > P_k < \chi_k \mid \phi_j > \qquad \text{(B-8)}$$

B.3 The Equation of Motion of the Density Matrix:

At a given instant we choose a basis set $(\chi_1 \chi_2 \ldots)$ in which $\bar{\bar{\rho}}$ is diagonal. The operator $\bar{\bar{\rho}}$ is then:

$$\bar{\bar{\rho}} = \sum_m \mid \chi_m > P_m < \chi_m \mid$$

Differentiating;

$$\frac{d}{dt}\bar{\bar{\rho}} = \sum_m \frac{d}{dt}\left(|\chi_m > P_m < \chi_m| \right) \qquad \text{(B-9)}$$

If we use the Schrödinger representation, the states are time dependent;

$$\frac{d}{dt}|\chi_m> = \frac{H}{i\hbar}|\chi_m>, \quad \frac{d}{dt}<\chi_m| = -\frac{1}{i\hbar}<\chi_m|H$$

The P_m are just numbers and do not vary with time, so equation (B-9) becomes:

$$\frac{h}{i}\frac{d}{dt}\bar{\bar{\rho}} = -[H\bar{\bar{\rho}} - \bar{\bar{\rho}}H] = -[H, \rho] \qquad \text{(B-10)}$$

B.4 Thermal Equilibrium:

What ever the cause of relaxation the system eventually reaches thermal equilibrium. At thermal equilibrium, the probability of a system being in the i^{th} state is given by Boltzmann's distribution law.

$$P_i = \frac{\exp(-E_i/kT)}{\sum_i \exp(-E_i/kT)} \qquad \text{(B-11)}$$

If $\bar{\bar{\rho}}$ is diagonal P_i is the same as the i^{th} diagonal element ρ_{ii}. The general expression for the density matrix operator $\bar{\bar{\rho}}_o$ at thermal equilibrium is:

$$\bar{\bar{\rho}}_o = \frac{\exp(-H/kT)}{\mathrm{tr}\,\exp(-H/kT)} \qquad \text{(B-12)}$$

APPENDIX C

THE MACROSCOPIC EQUATION

In order to obtain equation (2.13), begin by multiplying equation (2.6) by Q and taking the trace. We obtain:

$$\frac{dq^*}{dt} = -\,\mathrm{tr}\,\{\int_0^\infty d\tau\,\overline{[H_1^*(t),\ [H_1^*(t-\tau),\ \sigma^*(t)]]\ Q}\ \} \tag{C-1}$$

Now $[A,\ [B,C]] = [A,\ BC-CB]$

$$= ABC + CBA - ACB - BCA$$

Therefore,

$$\mathrm{tr}\,\{[H_1^*(t),\ [H_1^*(t-\tau),\ \sigma^*(t)]]Q\} =$$

$$\mathrm{tr}\,\{H_1^*(t)H_1^*(t-\tau)\sigma^*(t)\ Q + \sigma^*(t)H_1^*(t-\tau)H_1^*(t)Q - H_1^*(t)\sigma^*(t)H_1^*(t-\tau)Q - H_1^*(t-\tau)\sigma^*(t)H_1^*(t)Q\ \} \tag{C-2}$$

Now:

$$\mathrm{tr}\,\{ABCD\} = \mathrm{tr}\,\{BCDA\} = \mathrm{tr}\,\{CDAB\} = \mathrm{tr}\,\{DABC\} \tag{C-3}$$

Hence we may rewrite equation (C-2) as:

$$\mathrm{tr}\,\{[H_1^*(t),\ [H_1^*(t-\tau),\ \sigma^*(t)]]Q\} = -\,\mathrm{tr}\,\{[H_1^*(t-\tau),[H_1^*(t),Q]]\sigma^*\} \tag{C-4}$$

which is:

$$\mathrm{tr}\,\{[\mathcal{H}_1^*(t),\ [\mathcal{H}_1^*(t-\tau),\sigma^*(t)]]Q\} = -\ \mathrm{tr}\{A\sigma^*\}$$

where

$$A = \int_0^\infty d\tau\, \overline{[\mathcal{H}_1^*(t-\tau),\ [\mathcal{H}_1^*(t),\ Q]]} \tag{C-5}$$

and hence:

$$\frac{dq^*}{dt} = -\ \{a^* - a_o\}$$

APPENDIX D

COMMUTATORS

D.1 Dipolar Coupling:

$$[A^{(-1)},[A^{(1)},I_z + I'_z]] = [A^{(-1)},[I_zI'_+ + I_+I'_z,\ I_z + I'_z]\ ]$$

First evaluate:

$$[I_zI'_+ + I_+I'_z,\ I_z + I'_z] = [I_zI'_+,I_z] + [I_zI'_+,\ I'_z] + [I_+I'_z,I_z] + [I_+I'_z,I'_z]$$

$$= I_z[I'_+,I'_z] + I'_z[I_+,I_z]$$

$$= -\ I_zI'_+ - I'_zI_+$$

Now evaluate the remainder and obtain:

$$[A^{(-1)},[A^{(1)},I_z + I'_z]] = -[I_zI'_- + I_-I'_z,\ I_zI'_+ + I'_zI_+]$$

$$= -[I_zI'_-,I_zI'_+] - [I_zI'_-,I'_zI_+] - [I_-I'_z,I_zI'_+]$$

$$-\ [I_-I'_z,\ I'_zI_+]$$

which yields:

$$[A^{(-1)},[A^{(1)},I_z + I'_z]] = -\ I_z^2[I'_-,I'_+] - I'^2_z[I_-,I_+] - I_zI'_-I'_zI_+ + I'_zI_+I_zI'_-$$

$$-\ I_-I'_zI_zI'_+ + I_zI'_+I_-I'_z$$

The last four terms in above can be made to yield:

$$-\ [I_+I'_- + I_-I'_+]\ [I_z + I'_z]$$

Collecting terms and introducing a factor of α^2 which we dropped for convenience,

$$[A^{(-1)},[A^{(1)},I_z + I'_z]] = 2\alpha^2 I'_z I_z^2 + 2\alpha^2 I_z I_z'^2 - \alpha\ [I_+I'_- + I_-I'_+][I_z + I'_z]$$

Form now:

$$[A^{(-1)},[A^{(1)},I_z + I'_z]]^\dagger = 2\alpha^2 I'_z I_z^2 + 2\alpha^2 I_z I_z'^2 - \alpha[I_+I'_- + I_-I'_+]^\dagger[I_z + I'_z]$$

but,

$$[I_+I'_- + I_-I'_+]^\dagger = [I'_+I_- + I'_-I_+] = [I_+I'_- + I_-I'_+]$$

because I'_+I_- commutes. Therefore,

$$[A^{(-1)},[A^{(1)},I_z + I'_z]]^\dagger = [A^{(-1)},[A^{(1)}, I_z + I'_z]]$$

Now to evaluate:

$$[A^{(-2)},[A^{(2)},I_z + I'_z]]$$

Begin with:

$$[A^{(2)},I_z + I'_z] = [I_+I'_+, I_z + I'_z] = [I_+I'_+,I_z] + [I_+I'_+,I'_z] = -2\ I_+I'_+$$

Now multiply by 1/2 because of factor in $A^{(2)}$. We must now evaluate:

$$[A^{(-2)},I_+I'_+] = -[I_-,I_+]I'_-I'_+ - I_+I_-[I'_-, I'_+]$$

$$= 2\ I_zI'_-I'_+ - 2\ I_+I_-I'_z$$

Again, drop factor 2. Hence,

$$[A^{(-2)},I_+I'_+] = I_zI'_-I'_+ + I_+I_-I'_z .$$

but $I_-I_+ = I_x^2 + I_y^2 - I_z$; substituting we obtain:

$$[A^{(-2)}, I_+I'_+] = \alpha^2 I_z(I'^2_x + I'^2_y) + \alpha^2(I_x^2 + I_y^2)\, I'_z$$

where we have introduced a factor α^2 which was previously dropped for convenience.

D.2 Quadrupole Coupling:

We begin by evaluating:

$$[A^{(-1)}, [A^{(1)}, I_z]] = [I_zI_- + I_-I_z,\ [I_zI_+ + I_+I_z, I_z]]$$

First evaluate the inner commutator:

$$\begin{aligned}
[I_zI_+ + I_+I_z, I_z] &= I_zI_+I_z + I_+I_zI_z - I_z^2I_+ - I_zI_+I_z \\
&= I_z(I_zI_+ - I_+) + (I_zI_+ - I_+)I_z - I_z^2I_+ - I_z[I_zI_+ - I_+] \\
&= (I_z - 1)^2\, I_+ - I_z^2I_+ \\
&= (1 - 2I_z)\, I_+
\end{aligned}$$

We must now evaluate,

$$[I_zI_- + I_-I_z,\ (1 - 2I_z)\, I_+] = [(2I_z + 1)I_-,\ (1 - 2I_z)I_+]$$

$$\begin{aligned}
[(2I_z + 1)I_-, (1 - 2I_z)I_+] &= -\,[4I_z^2 + 4I_z + 1]I_-I_+ + [4I_z^2 - 4I_z + 1]I_+I_- \\
&= 4I_z^2[I_+, I_-] - 4I_z\,\{I_+, I_-\} + [I_+, I_-] \\
&= 8I_z^3 - 8I_z(I^2 - I_z^2) + 2I_z
\end{aligned}$$

and carrying through the numerical factor from $A^{(-1)}$ we get:

$$[A^{(-1)},[A^{(1)},I_z]] = 3/2\ \{16I_z^3 - I_z[8I(I + 1) - 2]\}$$

The commutator:

$$[A^{(-2)},[A^{(2)},I_z]] = [I_-^2,[I_+^2,I_z]]$$

First evaluate the inner commutator.

$$\begin{aligned}[I_+^2,I_z] &= I_+^2I_z - I_zI_+^2\\ &= I_+I_+I_z - I_zI_+^2\\ &= I_+(I_z - 1)I_+ - I_zI_+^2\\ &= (I_z - 2)I_+^2 - I_zI_+^2\\ &= -2I_+^2\end{aligned}$$

We now must evaluate (drop numerical factors for convenience):

$$\begin{aligned}[I_-^2,I_+^2] &= I_-^2I_+^2 - I_+^2I_-^2\\ &= I_-I_-I_+I_+ - I_+I_+I_-I_-\\ &= I^2[I_-,I_+] - I_-I_z(I_z + 1)I_+ + I_+I_z(I_z - 1)I_-\\ &= 2I^2I_z + (I_z^2 + 2)[I_+,I_-] - 3I_z\ \{I_-,I_+\}\\ &= 8I_z^3 + I_z\ (-8I^2 + 4)\end{aligned}$$

Carry through the numerical factors and obtain:

$$[A^{(-2)},[A^{(2)},I_z]] = 3/2\ (-16I_z^3 + I_z\ [16I(I + 1) - 8])$$

APPENDIX E

TENSOR OPERATORS AND SPHERICAL HARMONICS

To evaluate the various members of equation (2.48) begin by recalling:

$$Y_\ell^\ell(\theta,\phi) = (-1)^\ell \sqrt{\frac{(2\ell+1)!}{4\pi}} \; \frac{\quad}{2^\ell \ell!} \; \left(\frac{x+iy}{r}\right)^\ell \tag{E-1}$$

Furthermore,

$$\begin{aligned} x + iy &= r \sin\theta \, e^{i\phi} \\ x - iy &= r \sin\theta \, e^{-i\phi} \\ z &= r \cos\theta \end{aligned} \tag{E-2}$$

The above are obtained by substituting :

$$\begin{aligned} x &= r \sin\theta \cos\phi \\ y &= r \sin\theta \sin\phi \\ z &= r \cos\theta \end{aligned}$$

The following will also prove useful:

$$\begin{aligned} L_+ = L_x + iL_y &= e^{i\phi} \left(\frac{\partial}{\partial\theta} + i \cot\theta \frac{\partial}{\partial\phi}\right) \\ L_- = L_x - iL_y &= e^{-i\phi} \left(- \frac{\partial}{\partial\theta} + i \cot\theta \frac{\partial}{\partial\phi}\right) \end{aligned} \tag{E-3}$$

and

$$L_- Y_\ell^m = H_\ell^m \, Y_\ell^{m-1} \tag{E-4}$$

where

$$H_\ell^m = \sqrt{(\ell - m + 1)(\ell + m)}$$

We begin by first obtaining the operator $A_2{}^2$. Now by equation (E-1):

$$Y_2{}^2(\theta,\phi) = (-1)^2 \sqrt{\frac{(2.2 + 1)!}{4\pi}} \; \frac{1}{2^2 2!} \; \left(\frac{x + iy}{r}\right)^2$$

and hence,

$$A_2{}^2 = \sqrt{\frac{4\pi}{(2.2 + 1)}} \; \sum_i e_i r^2 (-1)^2 \sqrt{\frac{(2.2 + 1)!}{4\pi}} \; \frac{1}{2^2 2!} \left(\frac{x_i + iy_i}{r}\right)^2$$

from which

$$A_2{}^2 = \frac{\sqrt{6}}{4} \sum_i e_i (x_i + iy_i)^2$$

Finally, observe

$$Y_\ell^{-m}(\theta,\phi) = (-)^m \, Y_\ell^{m*}(\theta,\phi) \qquad \text{(E-4)}$$

and hence;

$$A_2^{-2} = \frac{\sqrt{6}}{4} \sum_i e_i (x_i - iy_i)^2$$

In order to get A_2^1 we need $Y_2^1(\theta,\phi)$. From equation (E-4):

$$Y_2^1 = \frac{L_- Y_2{}^2}{H_2{}^2} = \frac{L_- Y_2{}^2}{2}$$

Now calculate $L_- Y_2{}^2$.

From equation (E-3) we may write:

$$L_-Y_2^{\,2} = e^{-i\phi}\left(-\frac{\partial}{\partial\theta} + i\cot\frac{\partial}{\partial\phi}\right)\left((-1)^2\sqrt{\frac{(2.2+1)!}{4\pi}}\ \frac{1}{2^2 2!}\ \frac{r^2\sin^2\theta e^{2i\phi}}{r^2}\right)$$

or dropping the numerical factors for now,

$$L_-Y_2^{\,2} \cong e^{-i\phi}\left(-\frac{\partial}{\partial\theta} + i\cot\theta\,\frac{\partial}{\partial\phi}\right)(\sin^2\theta e^{2i\phi})$$

$$= \frac{-4}{r^2}\,z(x+iy)$$

and

$$\frac{L_-Y_2^{\,2}}{2} = -\sqrt{\frac{(2.2+1)!}{4\pi}}\ \frac{1}{4}\ \frac{z}{r^2}\,(x+iy) = Y_2^1$$

Therefore:

$$A_2^{\,1} = -\sqrt{\frac{4\pi}{(2.2+1)}}\ \sum_i e_i r_i^{\,2}\sqrt{\frac{(2.2+1)!}{4\pi}}\ \frac{1}{4}\ \frac{z_i}{r_i^{\,2}}\,(x_i+iy_i)$$

or

$$A_2^{\,1} = -\frac{\sqrt{6}}{2}\sum_i e_i z_i(x_i+iy_i)$$

By equation (e-4):

$$A_2^{-1} = -\frac{\sqrt{6}}{2}\sum_i e_i z_i(x_i-iy_i)$$

To obtain $A_2^{\,0}$ we need $Y_2^{\,0}$.

From equation (E-4) we have:

$$Y_2{}^0 = \frac{L_-Y_2^1}{\sqrt{6}}$$

Now calculate $L_-Y_2^1$.

From equation (E-3) we again may write:

$$L_-Y_2^1 = e^{-i\phi}\left(-\frac{\partial}{\partial\theta} + i \cot\theta \frac{\partial}{\partial\phi}\right)\left(-\frac{1}{4}\sqrt{\frac{(2.2+1)!}{4\pi}}\ z\ \frac{(x+iy)}{r^2}\right)$$

or dropping the numerical factors for now:

$$L_-Y_2{}^1 \cong e^{-i\phi}\left(-\frac{\partial}{\partial\theta} + i \cot\theta \frac{\partial}{\partial\phi}\right)\left(\frac{\sin 2\theta}{2}\ e^{i\phi}\right)$$

$$\cong -\ (3 \cos^2\theta - 1)$$

And finally,

$$Y_2{}^0 = \frac{L_-Y_2^1}{\sqrt{6}} = \sqrt{\frac{(2.2+1)!}{4\pi}}\ \frac{1}{4\sqrt{6}}\ (3\cos^2\theta - 1)$$

Therefore,

$$A_2{}^0 = \sqrt{\frac{4\pi}{(2.2+1)}}\ \sum_i e_i r_i{}^2 \sqrt{\frac{(2.2+1)!}{4\pi}}\ \frac{1}{4\sqrt{6}}\ (3\cos^2\theta - 1)$$

$$= \frac{1}{2}\ \sum_i\ e_i(3z_i{}^2 - r_i{}^2)$$

REFERENCES

1. Purcell, E. M., Torrey, H. C. and Pound, R. V., 1946, Phys. Rev., 69, 37.
2. Bloch, F., Hansen, W. W., and Packard, M. E., 1946, Phys. Rev., 69, 127.
3. Matthias, B. T., and Remeika, J. P., 1956, Phys. Rev., 103, 262.
4. Pepinsky, R., and Jona, F., 1957, Phys. Rev., 105, 344.
5. Hoshino, S., Vedam, K., Okaya, Y., and Pepinsky, R., 1958, Phys. Rev., 112, 405.
6. Strukov, B. A., Gavrilyuk, N. D., and Koptsik, V. A., 1961, Kristallografia, 6, 625.
7. Blinc, R., Levstek, I., 1960, J. Phys. Chem. Solids, 12, 295.
8. Richards, R. E., and Schaefer, T., 1961, Trans. Faraday Soc., 57, 210.
9. Miller, S. R., Blinc, R., Brenman, M., and Waugh, J. S., 1962, Phys. Rev., 126, 528.
10. O'Reilly, D. E., and Tsang, T., 1967, J. Chem. Phys., 46, 1291.
11. O'Reilly, D. E., Peterson, E. M., and Tsang, T., 1967, Phys. Rev. 160, 333.
12. Schlemper, E. O., and Hamilton, W. C., 1966, J. Chem. Phys., 44, 4498.
13. Rush, J. J., and Taylor, T. I., 1965, Inelastic Scattering Neutrons Solids Liquids, Proc. Symp. 3rd Bombay, India, 2, 333.

14. Abragam, A., 1961, The Principles of Nuclear Magnetism, Oxford University Press, Ch. VIII.

15. Van Vleck, J. H., 1948, Phys. Rev., 74, 1168.

16. Bloembergen, N., Purcell, E. M., and Pound, R. V., 1948, Phys. Rev., 73, 679.

17. Slichter, C. P., 1963, Principles of Magnetic Resonance, Harper and Row, Ch. V.

18. Torrey, H. C., 1949, Phys. Rev., 76, 1059.

19. Linder, S., 1957, J. Chem. Phys., 26, 900.

20. Wyckoff, R. W. G., 1965, Crystal Structures, Interscience, Ch. VIII-B.

21. Okaya, Y., Vedam, K., and Pepinsky, R., 1958, Acta Cryst., 11, 307.

22. Kydon, D., Pintar, M. and Petch, H. E., 1967, J. Chem. Phys, 47, 1185.

23. Trappeniers, N. J., Gerritsma, C. J., and Oosting, P. H., 1964, Physica, 30, 997.

24. Rabideau, S. W., and Waldstein, P., 1965, J. Chem. Phys., 42, 3822.

25. Chiba, T., 1962, J. Chem. Phys., 36, 1122.

26. Bersohn, R., and Gutowsky, H. S., 1954, J. Chem. Phys., 22, 651.

27. Tomita, K., 1953, Phys. Rev., 89, 429.